



Telemark University College

Faculty of technology

M.Sc. Programme

Master's Thesis FMH606 Spring 2013

Candidate: Tommy Fredriksen

Title: Wind Energy; CFD simulation
of wakes and wind turbine
forces



Faculty of Technology

Address: Kjølnes Ring 56, N-3914 Porsgrunn, Norway, tel: +47 35 57 50 00, fax: +47 35 55 75 47

Lower Degree Programmes - M.Sc. Programmes - Ph.D. Programmes



Telemark University College

Faculty of Technology

M.Sc. Programme

MASTER'S THESIS, COURSE CODE FMH606

Student: Tommy Fredriksen

Thesis title: Wind Energy; CFD simulation of wakes and wind turbine forces

Signature:

Number of pages: 75

Keywords: CFD, Wind Power, OpenFOAM, ALM, Wmware
Matlab
.....

Supervisor: Knut Vågsæther sign.:

2nd Supervisor: Eirik Manger sign.:

Censor: <name> sign.:

External partner: Siri M. Kalvig sign.:

Availability: Open

Archive approval (supervisor signature): sign.: **Date :**

Abstract:

Wind power is a clean and renewable energy source, which plays an important role in the world's energy landscape. When developing a wind farm it is beneficial to analyze the flow pattern in order to maximize the total performance of the wind farm, it is also important to predict wake patterns to prevent structural damage on downstream turbines. Traditional fully detailed CFD models will be very computational heavy to utilize for such analysis. In order to perform an analysis with reasonable computational cost, a simplified model is needed. The actuator line model is a simplified model, which is available and implemented in OpenFOAM. Since OpenFOAM is an open source software, it is possible to modify the code as needed. The model was tested, and the results were compared to experimental results from a workshop done by NTNU. In order to achieve the results close to the reference data, the solver needed to be modified. The implicit solver proposed, was able to get close to the reference data for the power and thrust calculations. The actuator line model was useful to predict the wake and calculate the power and thrust, but require a significant amount of tuning to achieve the desired results. The model is sensitive to parameter changes, and will be difficult to verify without experimental data.

Telemark University College accepts no responsibility for results and conclusions presented in this report.

Table of contents

1	INTRODUCTION	11
1.1	BACKGROUND	11
1.2	RELATED WORK.....	11
2	PROBLEM DESCRIPTION	12
3	THEORY.....	13
3.1	FLUID DYNAMICS.....	13
3.1.1	<i>Airfoils</i>	13
3.1.2	<i>Torque</i>	13
3.1.3	<i>Wind turbines</i>	14
3.2	ACTUATOR LINE MODEL	14
3.2.1	<i>Original solver</i>	16
3.2.2	<i>Implicit solver</i>	17
4	METHODS.....	19
4.1	OPENFOAM.....	19
4.2	SIMULATION SETUP	20
5	RESULTS.....	23
5.1	SIMULATION RESULTS	24
5.1.1	<i>Case 1</i>	24
5.1.2	<i>Case 2</i>	26
5.1.3	<i>Case 3</i>	29
5.1.4	<i>Case 4</i>	31
5.1.5	<i>Case 5</i>	33
5.1.6	<i>Case 6</i>	36
5.1.7	<i>Case 7</i>	38
5.1.8	<i>Case 8</i>	41
5.1.9	<i>Case 9</i>	44
5.1.10	<i>Case 10</i>	45
5.1.11	<i>Case 11</i>	48
5.1.12	<i>Case 12</i>	50
5.1.13	<i>Case 13</i>	52
5.1.14	<i>Case 14</i>	54
5.1.15	<i>Case 15</i>	56
5.1.16	<i>Case 16</i>	57
5.1.17	<i>Case 17</i>	58
5.1.18	<i>Case 18</i>	60
6	DISCUSSION.....	63
7	CONCLUSION	64
	REFERENCES.....	65
	APPENDICES	66

APPENDIX 1..... 67
APPENDIX 2..... 68
APPENDIX 3..... 70
APPENDIX 4..... 72
APPENDIX 5..... 74

Preface

This thesis is the final assignment for the master program, energy and environmental technology at Telemark university collage. The work was done over one semester in the spring of 2013.

I would like to thank Eirik Manger for excellent support and follow up, and thanks to Acona Flow technology in Skien for an office place and a considerable amount of coffee. And a thank to Knut Vågsæther for constructive discussions, and support. Thanks to Siri Kalvig for the possibility to contribute to ongoing research activities and the support to attend Deepwind 2013 in Trondheim. Also thanks to Anne mette Nodedal, student at NTNU for useful discussions and input. And thanks to Roy Stenbro at IFE for access to computing resources.

Porsgrunn 05.06.13

Tommy Fredriksen

Nomenclature

Symbols

ε	Smoothing factor in the Gaussian distribution [m]
Cl	Lift coefficient [-]
Cd	Drag coefficient [-]
a	Radius from rotation point [m]
F	Force [N]
T	Torque [Nm]
V	Fluid velocity [m/s]

Abbreviations

ALM	Actuator line model
CFD	Computational fluid dynamics
IEA	International Energy Agency
LES	Large eddy simulation
OpenFOAM	Open Field Operation and Manipulation
PISO	Pressure Implicit with Splitting of Operators
SOWFA	Simulator for Offshore Wind Farm Applications

Overview of figures

- Figure 3-1 Illustration of an airfoil with lift and drag vectors 13
- Figure 3-2 Illustration of a wind turbine 14
- Figure 3-3 The main functions in the ALM 15
- Figure 3-4 Figure showing the Gaussian smoothing function when epsilon = 1 16
- Figure 3-5 Original code structure for the PISO implementation in OpenFOAM, there are two modes shown, old and new position..... 17
- Figure 3-6 Implicit code structure for the PISO implementation in OpenFOAM 18
- Figure 4-1 Screenshot of ParaView 20
- Figure 4-2 Dimensions of the wind tunnel used in the simulation..... 21
- Figure 4-3 Lift and drag coefficient for the NREL S628 21
- Figure 4-4 Blade profile for the NREL S628 22
- Figure 5-1 Grid in the center plane for case1 24
- Figure 5-2 Case profile for case 1 25
- Figure 5-3 Velocity contour in the center plane through the rotor for case 1 25
- Figure 5-4 Body force distribution at the rotor plane for case 1 26
- Figure 5-5 Velocity profile in the wake at 1,3 and 5 rotor diameters downstream from the rotor for case 1 26
- Figure 5-6 Case profile for case 2 27
- Figure 5-7 Velocity contour in the center plane through the rotor for case 2 27
- Figure 5-8 Body force distribution at the rotor plane for case 2 28
- Figure 5-9 Power and thrust graphs for case 2 28
- Figure 5-10 Velocity profile in the wake at 1,3 and 5 rotor diameters downstream from the rotor for case 2..... 29
- Figure 5-11 Case profile for case 3 29
- Figure 5-12 Velocity contour in the center plane through the rotor for case 3 30
- Figure 5-13 Body force distribution at the rotor plane for case 3 30
- Figure 5-14 Power and thrust graphs for case 3 30
- Figure 5-15 Velocity profile in the wake at 1,3 and 5 rotor diameters downstream from the rotor for case 3..... 31
- Figure 5-16 Case profile for case 4 31
- Figure 5-17 Velocity contour in the center plane through the rotor for case 4 32
- Figure 5-18 Body force distribution at the rotor plane for case 4 32
- Figure 5-19 Power and thrust graphs for case 4 32

Figure 5-20 Velocity profile in the wake at 1,3 and 5 rotor diameters downstream from the rotor for case 4.....	33
Figure 5-21 Grid in the center plane for case 5.....	33
Figure 5-22 Case profile for case 5.....	34
Figure 5-23 Velocity contour in the center plane through the rotor for case 5.....	34
Figure 5-24 Body force distribution at the rotor plane for case 5.....	35
Figure 5-25 Power and thrust graphs for case 5.....	35
Figure 5-26 Velocity profile in the wake at 1,3 and 5 rotor diameters downstream from the rotor for case 5.....	36
Figure 5-27 Case profile for case 6.....	36
Figure 5-28 Velocity contour in the center plane through the rotor for case 6.....	37
Figure 5-29 Body force distribution at the rotor plane for case 6.....	37
Figure 5-30 Power and thrust graphs for case 6.....	37
Figure 5-31 Velocity profile in the wake at 1,3 and 5 rotor diameters downstream from the rotor for case 6.....	38
Figure 5-32 Case profile for case 7.....	39
Figure 5-33 Velocity contour in the center plane through the rotor for case 7.....	39
Figure 5-34 Body force distribution at the rotor plane for case 7.....	40
Figure 5-35 Power and thrust graphs for case 7.....	40
Figure 5-36 Velocity profile in the wake at 1,3 and 5 rotor diameters downstream from the rotor for case 7.....	41
Figure 5-37 Grid in the center plane for case 8.....	41
Figure 5-38 Case profile for case 8.....	42
Figure 5-39 Velocity contour in the center plane through the rotor for case 8.....	42
Figure 5-40 Body force distribution at the rotor plane for case 8.....	43
Figure 5-41 Power and thrust graphs for case 8.....	43
Figure 5-42 Velocity profile in the wake at 1,3 and 5 rotor diameters downstream from the rotor for case 8.....	44
Figure 5-43 Case profile for case 9.....	44
Figure 5-44 Power and thrust graphs for case 9.....	45
Figure 5-45 Velocity profile in the wake at 1,3 and 5 rotor diameters downstream from the rotor for case 9.....	45
Figure 5-46 Grid in the center plane for case 10.....	45
Figure 5-47 Case profile for case 10.....	46
Figure 5-48 Velocity contour in the center plane through the rotor for case 10.....	46

Figure 5-49 Body force distribution at the rotor plane for case 10	47
Figure 5-50 Power and thrust graphs for case 10.....	47
Figure 5-51 Velocity profile in the wake at 1,3 and 5 rotor diameters downstream from the rotor for case 10.....	48
Figure 5-52 Case profile for case 11	48
Figure 5-53 Velocity contour in the center plane through the rotor for case 11	49
Figure 5-54 Body force distribution at the rotor plane for case 11	49
Figure 5-55 Power and thrust graphs for case 11	50
Figure 5-56 Velocity profile in the wake at 1,3 and 5 rotor diameters downstream from the rotor for case 11.....	50
Figure 5-57 Case profile for case 12	51
Figure 5-58 Velocity contour in the center plane through the rotor for case 12.....	51
Figure 5-59 Body force distribution at the rotor plane for case 12	52
Figure 5-60 Power and thrust graphs for case 12.....	52
Figure 5-61 Case profile for case 13	53
Figure 5-62 Body force distribution at the rotor plane for case 13	53
Figure 5-63 Power and thrust graphs for case 13.....	54
Figure 5-64 Case profile for case 14	55
Figure 5-65 Body force distribution at the rotor plane for case 14.....	55
Figure 5-66 Power and thrust graphs for case 14.....	55
Figure 5-67 Case profile for case 15	56
Figure 5-68 Body force distribution at the rotor plane for case 15	56
Figure 5-69 Power and thrust graphs for case 15.....	57
Figure 5-70 Case profile for case 16	57
Figure 5-71 Body force distribution at the rotor plane for case 16.....	58
Figure 5-72 Power and thrust graphs for case 16.....	58
Figure 5-73 Case profile for case 17	59
Figure 5-74 Body force distribution at the rotor plane for case 17	59
Figure 5-75 Power and thrust graphs for case 17.....	60
Figure 5-76 Case profile for case 18	60
Figure 5-77 Velocity contour in the center plane through the rotor for case 18.....	61
Figure 5-78 Body force distribution at the rotor plane for case 18.....	61
Figure 5-79 Power and thrust graphs for case 18.....	61

Figure 5-80 Velocity profile in the wake at 1,3 and 5 rotor diameters downstream from the rotor for case 18.....	62
--	----

Overview of tables

Table 5-1 List over simulations using the original solver.....	23
Table 5-2 List over simulations using the explicit solver.....	23
Table 5-3 Grid refinement limits for case 1.....	24
Table 5-4 Grid refinement limits for case 5.....	33
Table 5-5 Grid refinement limits for case 7.....	38
Table 5-6 Grid refinement limits for case 8.....	41
Table 5-7 Grid refinement limits for case 10.....	46

1 Introduction

Wind power is a clean and renewable energy source, which is growing in popularity all over the world. The installed capacity of wind power is growing faster each year and is starting to play an important role in the world's energy landscape. It is also an essential power source to reach 2 degree and 4 degree scenarios set by the IEA (1). Wind farms are now also been developed for offshore locations, which host an array of new challenges from operation and maintenance to ocean environment effects. When developing a wind farm on land or offshore it is beneficial to analyze the flow pattern in order to maximize the total performance of the wind farm. And to predict the wake patterns downstream from the turbine. In order to perform this analysis, a model of the wind turbine is needed. A fully detailed model will quickly be extremely costly to use for a large wind farm, therefore a simplified model is needed.

In this thesis, an ALM is used to simulate a small-scale wind turbine in a wind tunnel, and compare the results to experimental data. The ALM is a simplified model which is feasible to apply to wind farm analysis.

1.1 Background

This thesis is related to the study performed by Siri Kalvig, which is studying the influence of ocean waves on the turbine wake. And the downstream structural loading of this effect on the turbine and rotor structure.

In order to simulate the airflow around a wind turbine, the most obvious approach would be to model the full geometry of turbine. However, this would result in a very big model with a high number of control volumes, which will make simulation heavy. One possible simplification is to represent the turbine rotor with a line, and then use tabulated airfoil data to manipulate the air flow.

1.2 Related work

Sørensen and Shen (2) presented ALM, in there article. This model was applied on a 500kW Nordtank wind turbine, this model gave good results. This model used a cylindrical coordinate system. Matthew Churchfield (3) Implemented the ALM in OpenFOAM in order to simulate large cases, mainly wind farms. However the LES model which was used in the study is very heavy and makes the simulation take a lot of time. Niels Troldborg (4) used the ALM in his PHD thesis, which were implemented in EllipSYS3D and used LES model as well. Krogstad and Eriksen (5) hosted blind test 1, were the objective was to model a small turbine model operating in a wind tunnel.

2 Problem description

The main objective with this study is to investigate the ALM implemented in OpenFOAM, and to validate the model with the results from Blind test 1. Determine the model parameters that will give the closest results to the experimental data. In addition, if necessary modify the solver to improve the results. The first step is to implement the updated ALM model from the SOWFA library, and see if it will improve the result.

3 Theory

In this section, some fundamental theory related the ALM will be provided. This will include some fluid dynamics and an overview of the ALM code.

3.1 Fluid dynamics

Basic airfoil theory, torque and wind turbine operations will be presented in this chapter.

3.1.1 Airfoils

Airfoils are geometric shapes that can generate a lift force from a fluid flow. The main factors are angle of attack and fluid velocity. Airfoils are used as rotors for horizontal wind turbines. An illustration of an airfoil is show in Figure 3-1 showing the lift and drag vectors. The lift and drag can be calculated with equation (3-1) and (3-2).

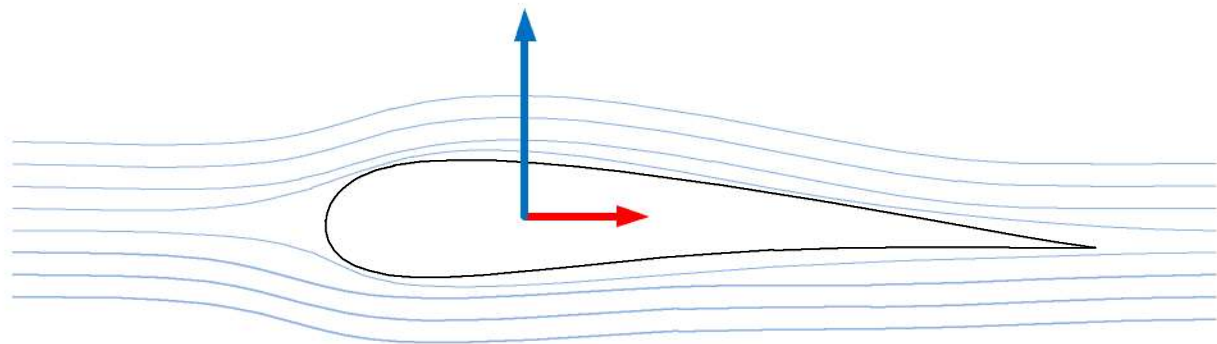


Figure 3-1 Illustration of an airfoil with lift and drag vectors

$$Lift = \frac{1}{2} \cdot Cl \cdot V_{mag}^2 \cdot Chord \cdot Width \quad (3-1)$$

$$Drag = \frac{1}{2} \cdot Cd \cdot V_{mag}^2 \cdot Chord \cdot Width \quad (3-2)$$

3.1.2 Torque

To calculate the torque generated by a rotor one can multiply the tangential force with radius of the force interaction point. The expression for torque is shown in equation (3-3).

$$T = F \cdot a \quad (3-3)$$

3.1.3 Wind turbines

Wind turbines are installations, which is converting kinetic energy from the wind into electrical energy. This is achieved with a big rotor acting on the wind flow, and then turning a generator. A wind turbine is shown in Figure 3-2

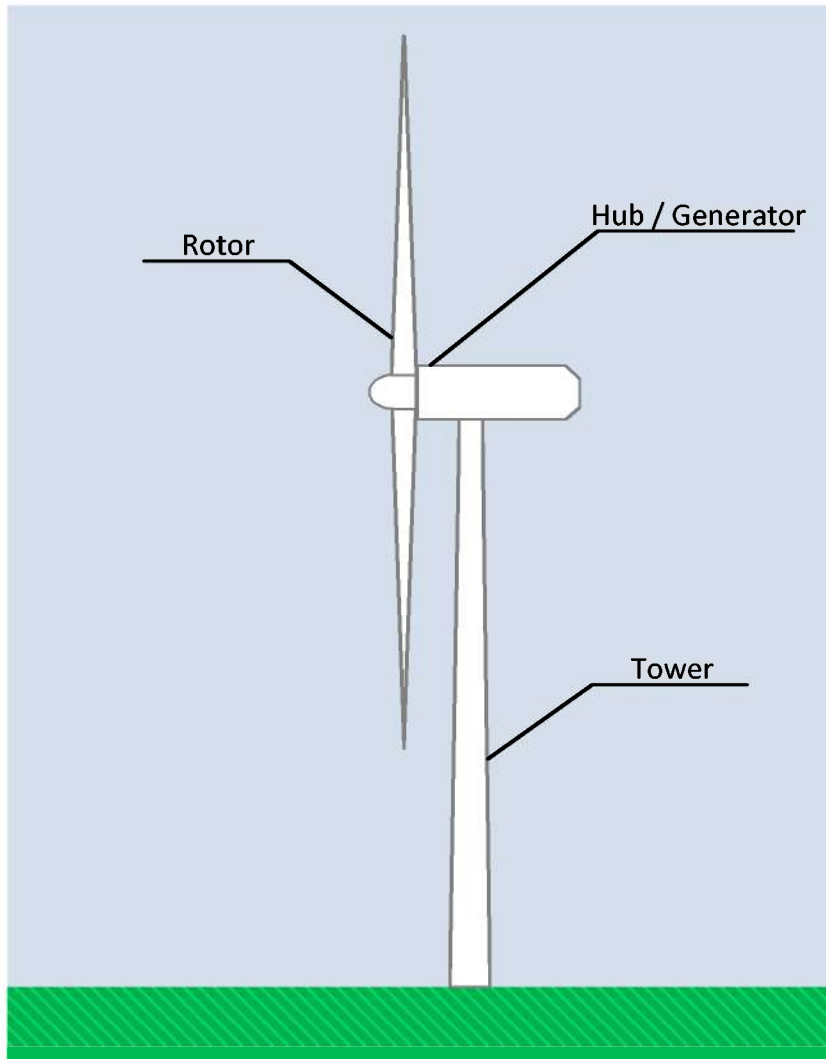


Figure 3-2 Illustration of a wind turbine

3.2 Actuator line model

The idea behind the ALM is to model the turbine rotor as simple lines rather than the full geometry. The lines are then introduced into the CFD grid. Each line is defined as multiple points. The force generated by the rotor is then calculated for each point. The force is then distributed back to the grid by a smoothing function.

The ALM code is implemented into the OpenFOAM environment with the PISO solver

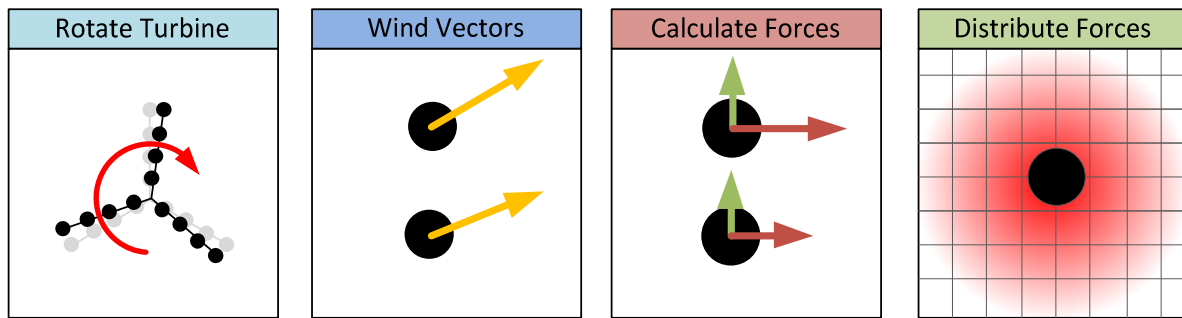


Figure 3-3 The main functions in the ALM

The ALM code can be described as four main functions. The first is *rotate turbine*, the second is *wind vectors*, the third is *calculate forces*, and the last is *distribute forces*. An illustration of the different functions can be found in Figure 3-3.

Rotate turbine

The Rotate turbine function calculate the Cartesian coordinates for the blade points based of the previous position and updated with the rotational speed.

Wind vectors

The read wind vectors function reads the magnitude of the velocity vector from the CFD grid where the blade point is located, this is the performed for each blade point.

Calculate forces

The calculate turbine forces function calculates the lift and drag force for each blade point, from the wind vectors and the tabulated blade data.

Distribute forces

The distribute forces function is distributing the calculated force onto the CFD grid to influence the flow. This is done with a three dimensional Gaussian function. The expression for the Gaussian function can be found in equation (3-5). The maximum distance from the blade point to the center of the influenced cell is calculated by equation (3-4), and is called the projection radius. Figure 3-4 shows the Gaussian distribution when epsilon is set to one. The selection of the epsilon factor is a critical process for achieving good results.

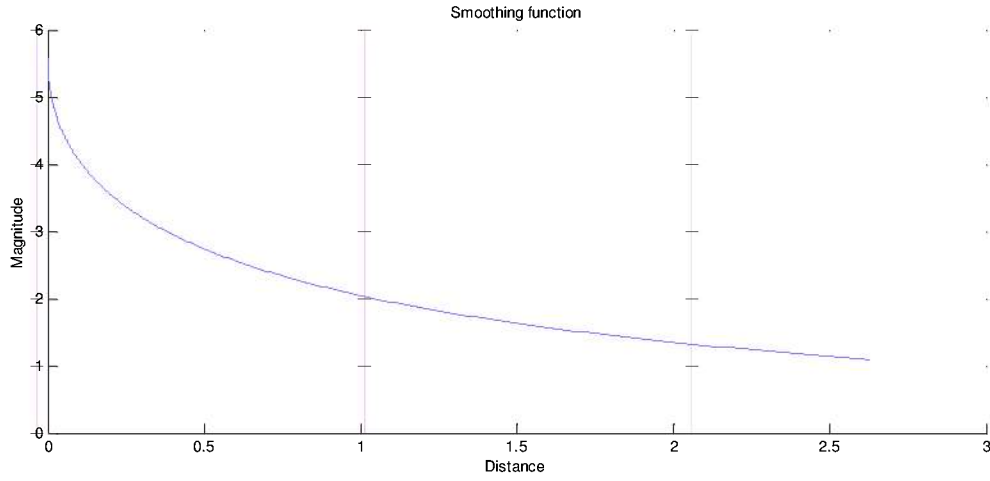


Figure 3-4 Figure showing the Gaussian smoothing function when epsilon = 1

$$F_{Cell} = F_{Point} \cdot \frac{\exp\left(-\sqrt{\frac{D}{\epsilon}}\right)}{\epsilon^3 \pi^{1.5}} \quad (3-4)$$

$$P_{radius} = \epsilon \sqrt{\log\left(\frac{1}{0.001}\right)} \quad (3-5)$$

3.2.1 Original solver

The ALM is implemented in the standard PISO solver (6) in OpenFOAM. The original ALM code is executed explicit, this however will create some instability when simulation with small time steps and when grid interference occurs. In order to improve the code the solver was made implicit by rearranging the ordering of the operations during a time. The update turbine function is called after the PISO loop. There is an option to use the old or the new position for calculation the wind vectors.

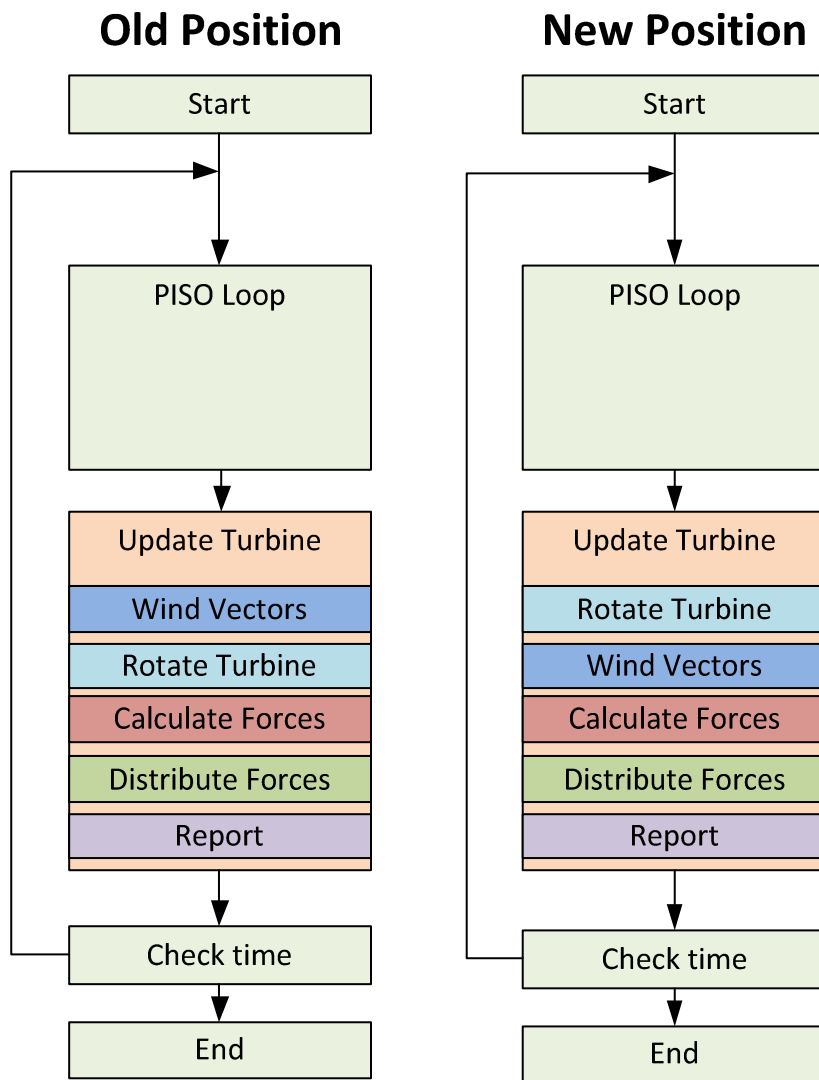


Figure 3-5 Original code structure for the PISO implementation in OpenFOAM, there are two modes shown, old and new position.

3.2.2 Implicit solver

An alternative structure is proposed, the main idea is that the force calculation is included in the PISO loop. The turbine force will then be part of the solving process of the conservation equations in the PISO loop. The structure of the implicit solver is shown in Figure 3-6.

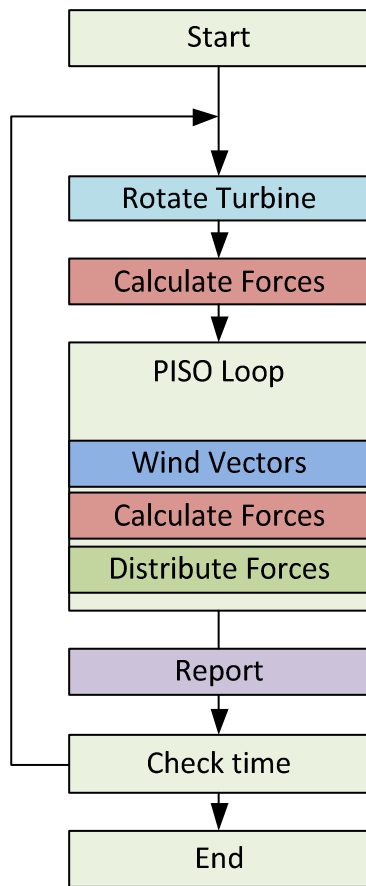


Figure 3-6 Implicit code structure for the PISO implementation in OpenFOAM

4 Methods

This section describes the methods and tools used in this thesis, first a brief introduction of OpenFOAM and ParaView then an overview of the simulation setup.

4.1 OpenFOAM

In order to simulate the wind tunnel, a CFD simulation software is needed. There are a few commercially available platforms, the most notable is Ansys fluent. However many industries are looking into open source solutions. One very popular Open source CFD platform is OpenFOAM. It can be downloaded for free from their website, and can also be modified to suite specialized needs. OpenFOAM have to run in a Linux environment, one possible implementation is to run it as a virtual machine running in a windows environment.

The main reason for choosing OpenFOAM is the unlimited capability to modify and add functionality, and it is free.

However OpenFOAM is not very user friendly, it does not have any graphical user interface. All the configuration is done by editing text files, and the output during the computation is only show in the terminal

OpenFOAM is a bit different from other CFD tools, one major notable difference is the case structure. The case structure is organized as configuration files, which have to be edited with a regular text editor, so in other words there are no specialized graphical user interface to work with.

In order to visualize the results, there is another tool available, which is called ParaView. ParaView have a graphical user interface, a screenshot is shown in Figure 4-1.

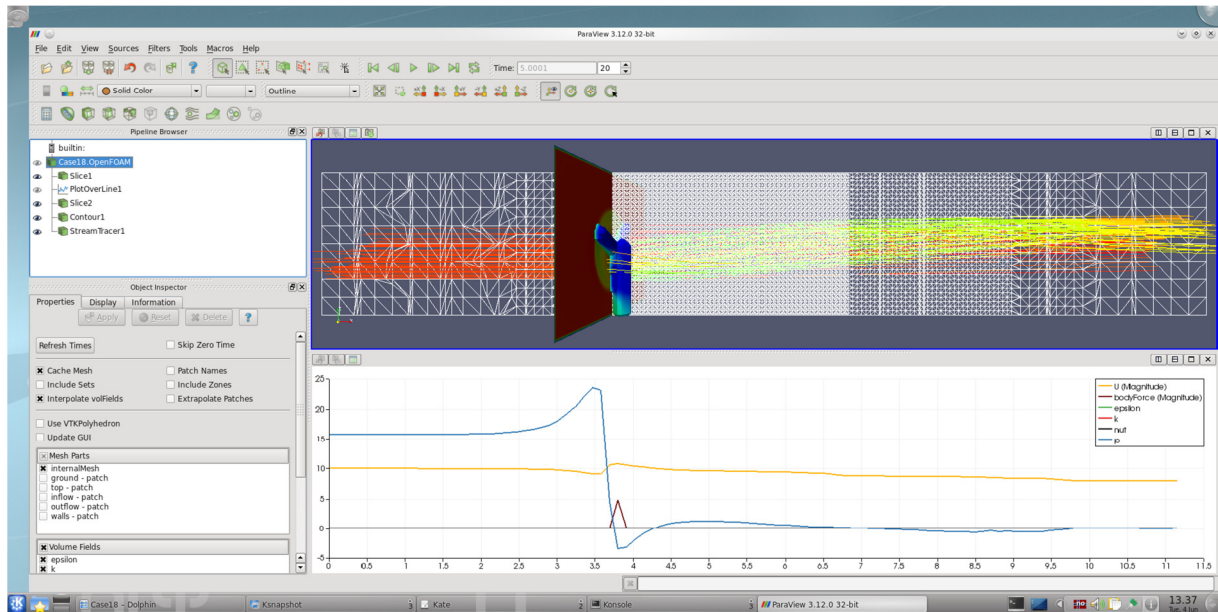


Figure 4-1 Screenshot of ParaView

4.2 Simulation setup

The simulation is based on the wind tunnel at NTNU in Trondheim with a small turbine model with NREL S628 blades. The blade profile can be found in Figure 4-4 and the drag and lift coefficients in Figure 4-3. The Center of the rotor is 0.817 m above the floor, the rotor diameter is 0.894 meters. For the simulation, the tip speed ratio was set to 6 since this was the design speed for the rotor, and should be the simplest to model. The simulation is based on blind test 1 and is modeled as close as possible. An illustration of the dimensions of the wind tunnel is shown in Figure 4-2. The turbulence model used for all cases except case 2, are the k-epsilon model, not to be confused with the Gaussian epsilon factor used in the ALM.

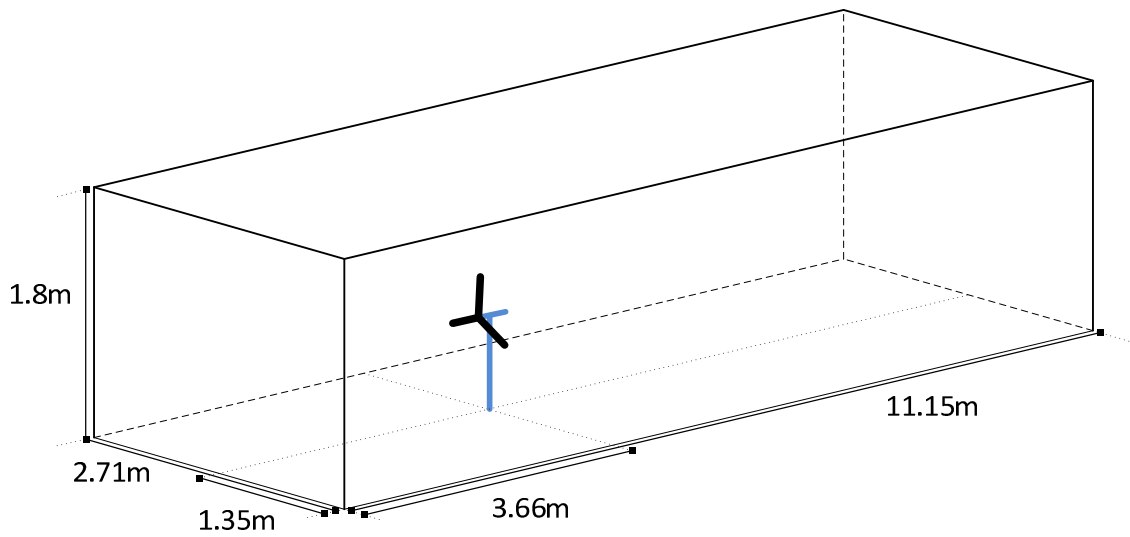


Figure 4-2 Dimensions of the wind tunnel used in the simulation

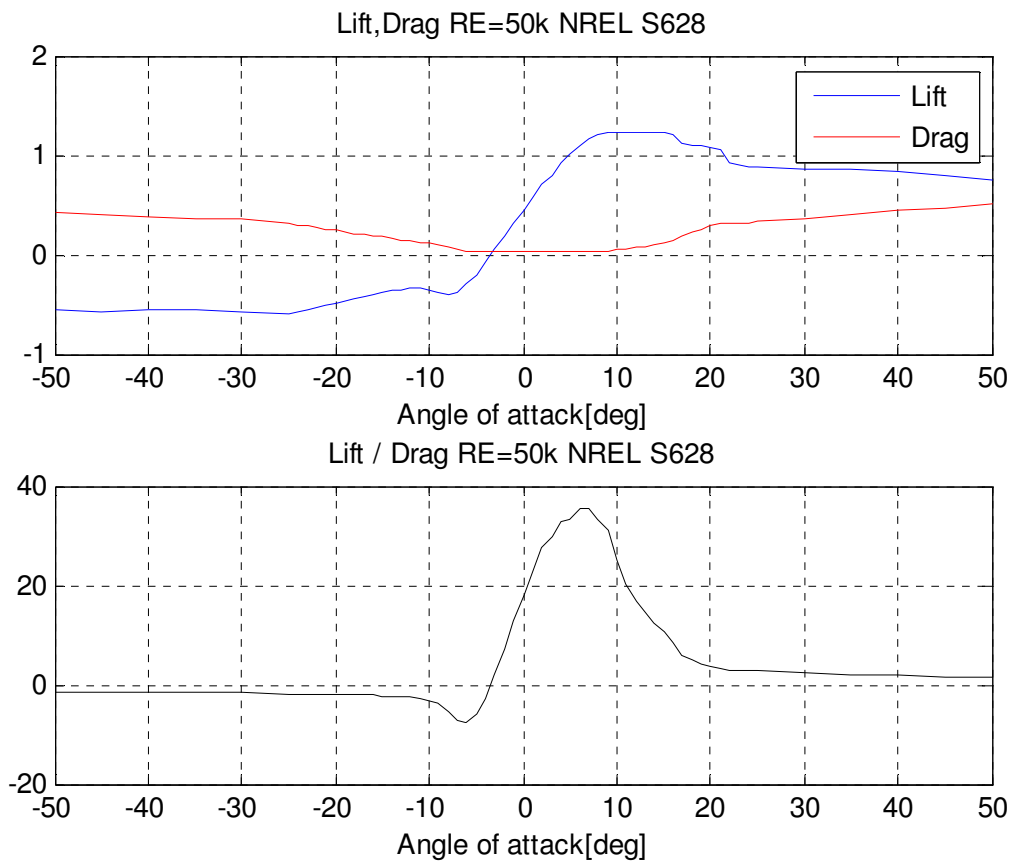


Figure 4-3 Lift and drag coefficient for the NREL S628

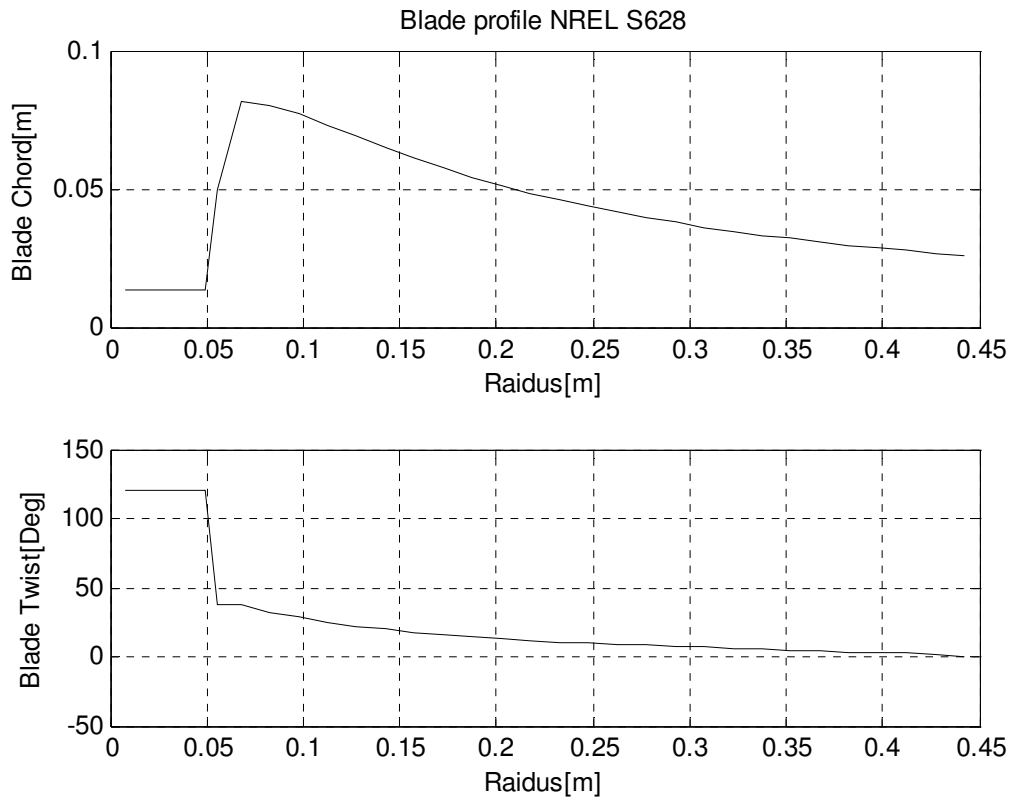


Figure 4-4 Blade profile for the NREL S628

The reference value for the power is calculated to be 177 w, and thrust to be 35.4 N from the results presented in blind test 1 (5).

5 Results

This section contains the results from the simulations, first there will be some initial results that were used to evaluate and tune the simulation parameters, then the final results will follow.

Table 5-1 List over simulations using the original solver

Name	dT[s]	Epsilon[m]	Base Mesh [xyz]	Blade Points
Case 1	0.001	0.039	45,18,18	12
Case 2	0.001	0.4	45,18,18	12
Case 3	0.001	0.04	45,18,18	12
Case 4	0.001	0.04	45,18,18	12
Case 5	0.0001	0.04	45,18,18	30
Case 6	0.001	0.004	45,18,18	30
Case 7	0.001	0.031	45,11,7	30
Case 8	0.001	0.018	75,18,12	30
Case 9	0.0004	0.0419	50,12,8	24
Case 10	0.00005	0.0101	50,12,8	100
Case 11	0.00007	0.012	50,12,8	90
Case 12	0.00009	0.012	50,12,8	80

Table 5-2 List over simulations using the explicit solver

Name	dT[s]	Epsilon[m]	Base Mesh [xyz]	Blade Points
Case 13	0.00009	0.012	50,12,8	80
Case 14	0.0003	0.04	50,12,8	75
Case 15	0.0003	0.03	50,12,8	75
Case 16	0.0003	0.02	50,12,8	75
Case 17	0.0003	0.023	50,12,8	75
Case 18	0.0003	0.026	50,12,8	75

5.1 Simulation results

This section contains results from all the simulations performed in this thesis. Some cases are only simulated for a shorter period of time, and is mainly aimed at the turbine power and thrust data from the ALM, these cases do not show the velocity contours since they are not properly developed.

In order to keep track of all the different parameters used in the simulations, a case profile was made for all the plots, the profile shows a number of key parameters together with the actual blade cord as reference, the main idea of this is to make it easier to visualize the difference between each case. The profile is composed of the epsilon factor, double the epsilon factor to compare with the blade chord, since the Gaussian distribution is both directions of the blade point. The projection radius is also included. The grid size is also shown, one point for each dimension. The next line is distance between each blade point, all simulations have used a uniform distribution of the blade points. The last line is the arc length of the jump that the root and tip blade point makes in one time step.

5.1.1 Case 1

This case is an initial case, which is similar to the simulations performed by Siri kalvig, and was mostly a system test and a reference to future simulations. The case profile is shown in Figure 5-2, from this profile we can see that the grid is not cubical, the dx is higher than the y and z dimensions. Also the 2x epsilon is about the same size as the thickest part of the actual blade. The arc length of the tip jump is big compared with the root jump, and is larger than epsilon.

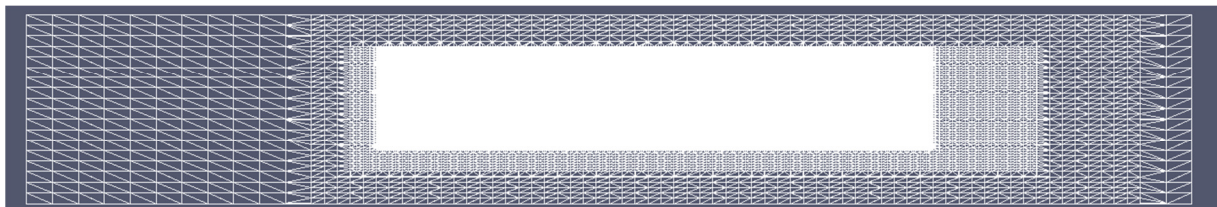


Figure 5-1 Grid in the center plane for case 1

The mesh used for this case was refined by the limits shown in Table 5-3, after the refinement the mesh is composed of 1233700 cells. The grid after the refinement is shown in Figure 5-1.

Table 5-3 Grid refinement limits for case 1

	X		Y		Z	
Level 1	-1.0	7.0	-1.3	1.3	0.0	1.8
Level 2	-0.6	6.0	-1.0	1.0	0.3	1.5
Level 3	-0.3	5.0	-0.7	0.7	0.5	1.5

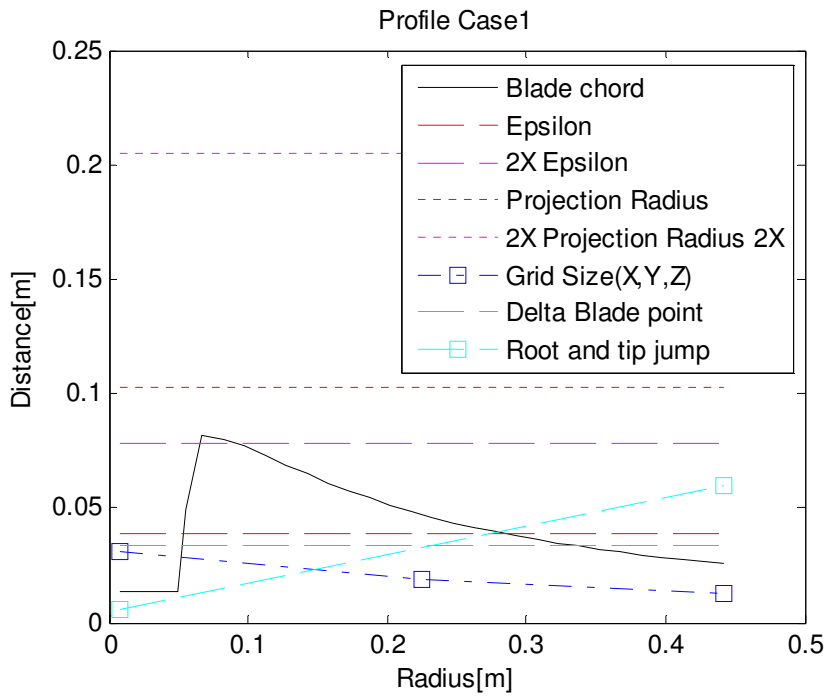


Figure 5-2 Case profile for case 1

From the velocity contour seen in Figure 5-3 we can see that the ALM has done influence to the flow field, however the flow through the center of the rotor is not influenced.

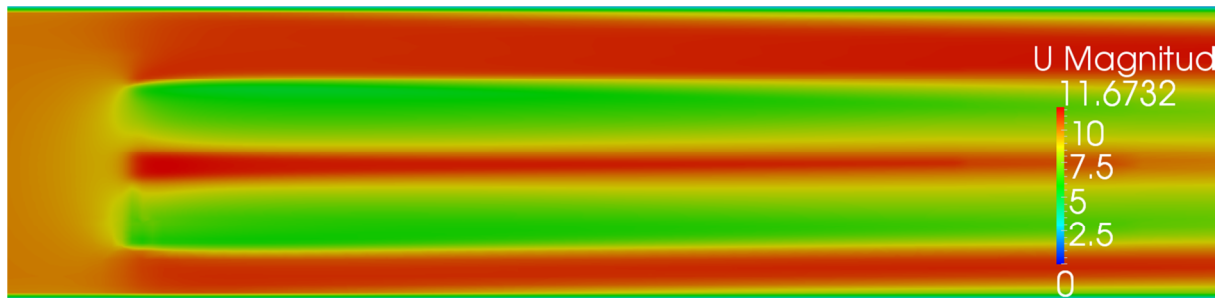


Figure 5-3 Velocity contour in the center plane through the rotor for case 1

From Figure 5-4 we can see the force distribution from the ALM to the CFD grid, it looks sensible, however note the difference on the blade pointing down, this is caused by a meshing error which was corrected later.

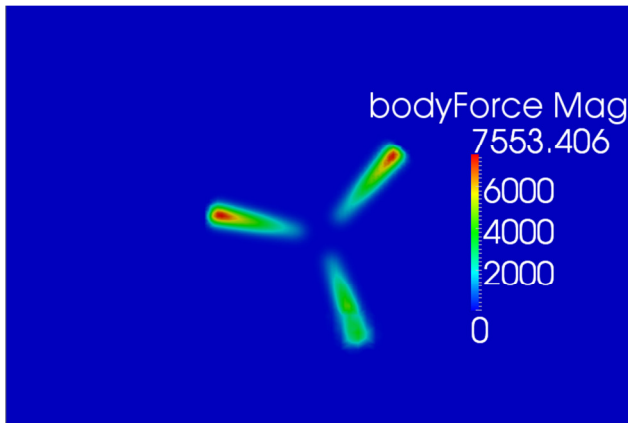


Figure 5-4 Body force distribution at the rotor plane for case 1

The velocity profiles for one, three and 5 diameters behind the rotor are found in Figure 5-5. Here we can see that the velocity on the side of the rotor and the tip have a quite good correlation, and the root velocity is too high.

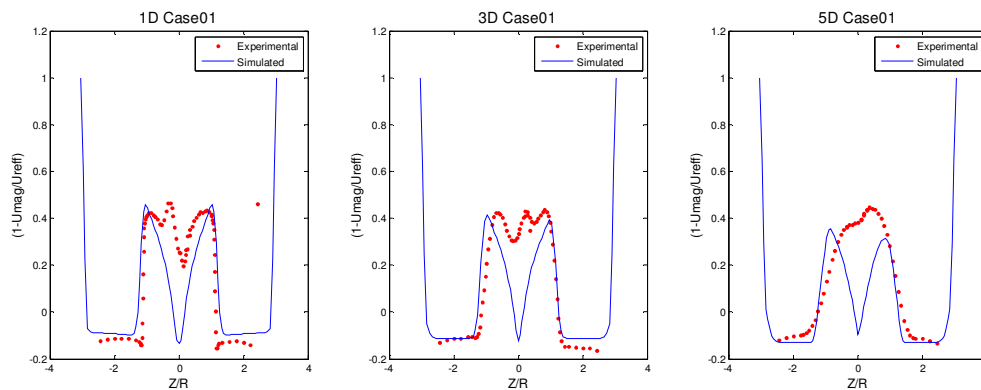


Figure 5-5 Velocity profile in the wake at 1,3 and 5 rotor diameters downstream from the rotor for case 1

5.1.2 Case 2

This case is the first to use the new SOWFA library, however there were some issues within the code with a name conflict. This with was omitted by disabling the turbulence model for the simulation. From the case profile shown in Figure 5-6 we can see that the epsilon value for this case is very high. The motivation behind selecting this value was to get an extreme case and see how the model responded. The rest of the parameters were unchanged from the previous case. The mesh used is the same as for case 1.

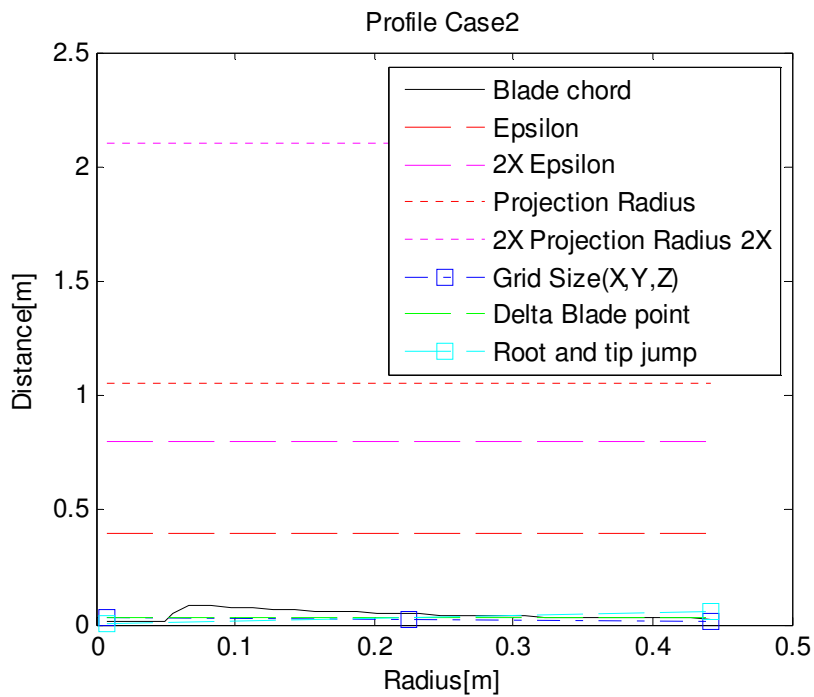


Figure 5-6 Case profile for case 2

In the velocity contour in Figure 5-7 we can see the influence is very smooth, and there is no center flow with higher velocity.

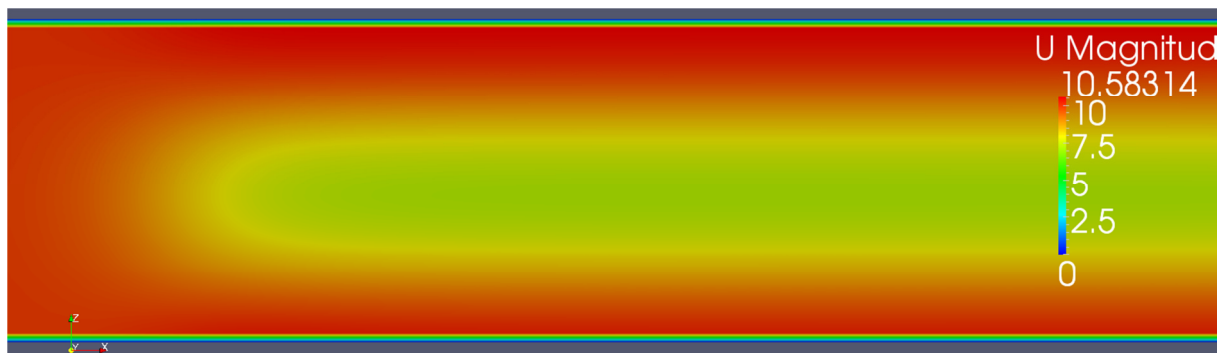


Figure 5-7 Velocity contour in the center plane through the rotor for case 2

The distribution of body forces is shown in Figure 5-8. Here we can see that the body forces are distributed over a large number of cells, and the value range is very low.

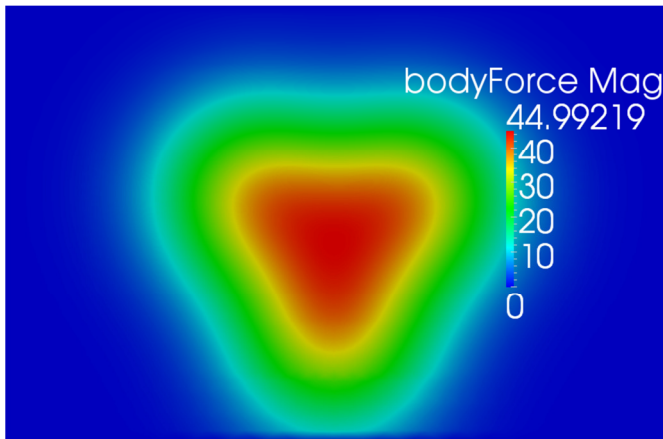


Figure 5-8 Body force distribution at the rotor plane for case 2

From the ALM we can read out the power and thrust calculated for the rotor, the data is shown in Figure 5-9. Here we can see that both the power and thrust have a high initial value, and is the decreasing over time until settling at a stable value. When plotting power against the blade angle we can see that it is quite smooth, however far above the reference value. And the same for the thrust.

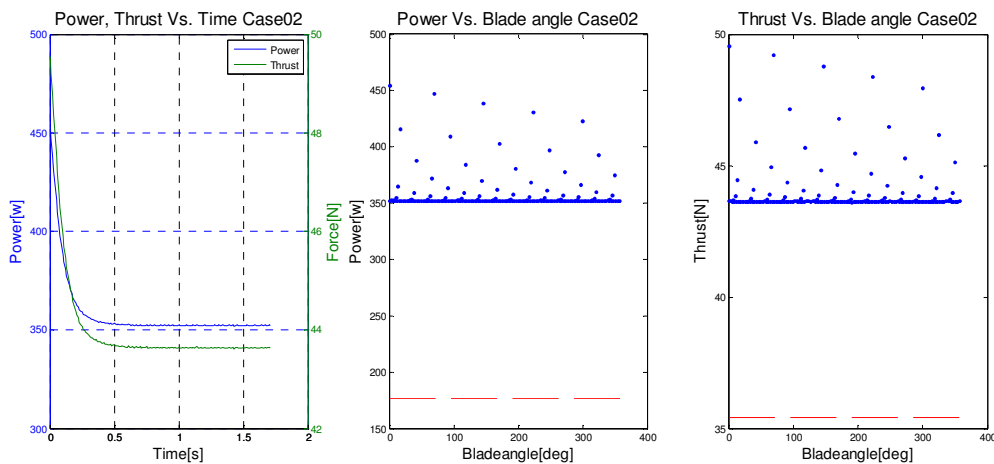


Figure 5-9 Power and thrust graphs for case 2

The velocity profiles for 1, 3 and 5 diameters behind the rotor are found in Figure 5-10. This case has poor correlation with the experimental data.

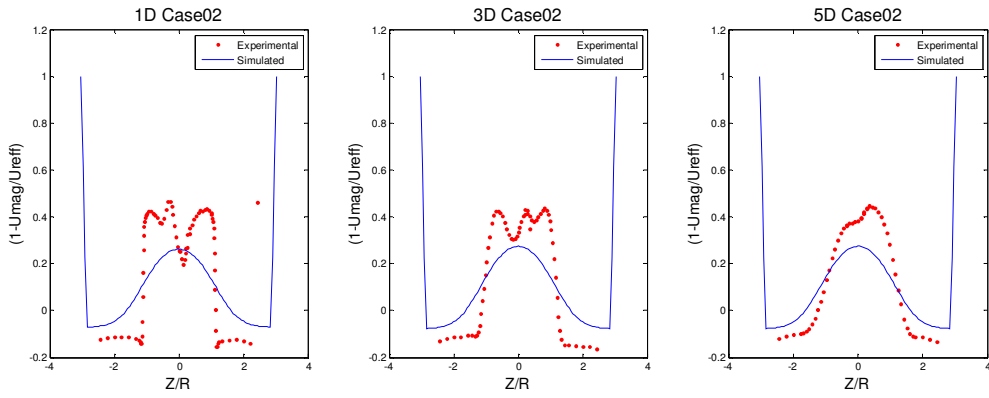


Figure 5-10 Velocity profile in the wake at 1,3 and 5 rotor diameters downstream from the rotor for case 2

5.1.3 Case 3

For this case, new airfoil data was used, and the conflict regarding the turbulence model has been resolved, so the turbulence model is working properly. The case profile is shown in Figure 5-11. The epsilon is now changed to a more reasonable value of 0.04.

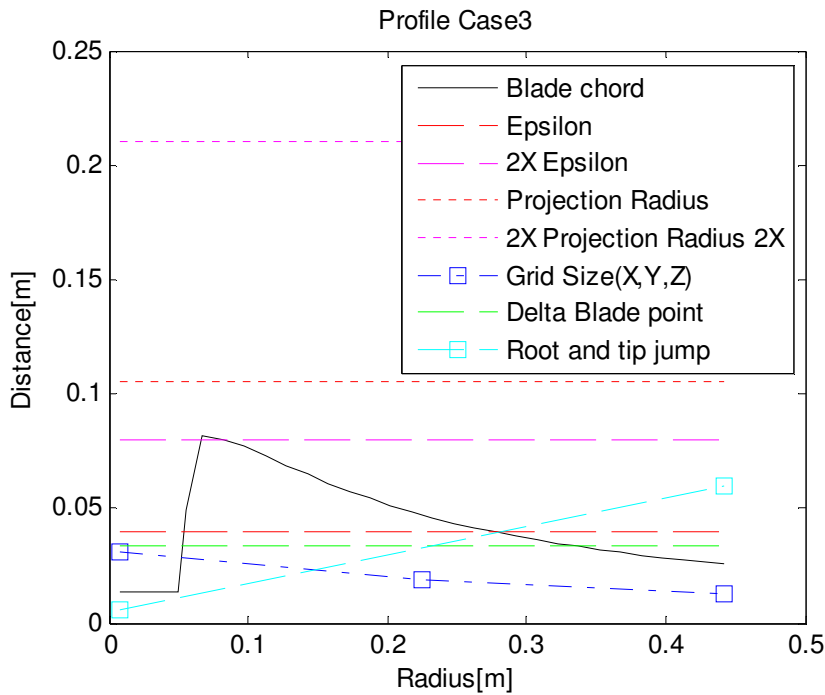


Figure 5-11 Case profile for case 3

The velocity contour is shown in Figure 5-12, this contour is similar to Case 1.

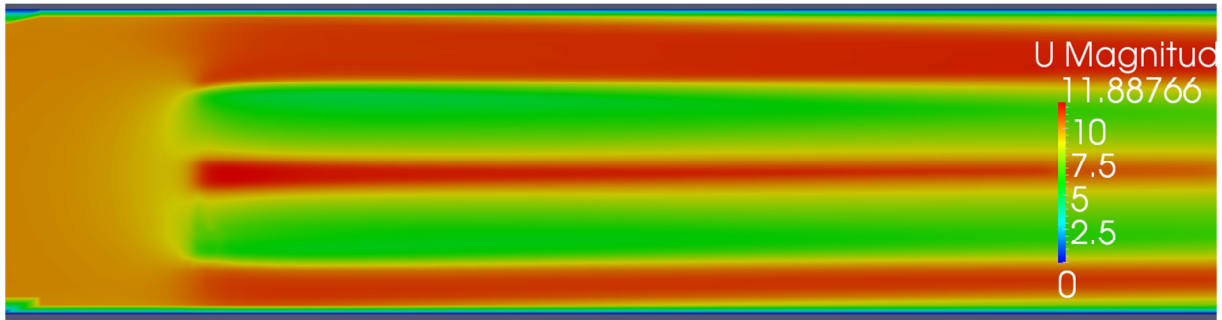


Figure 5-12 Velocity contour in the center plane through the rotor for case 3

The force distribution is shown in Figure 5-13, it also has the mesh error.

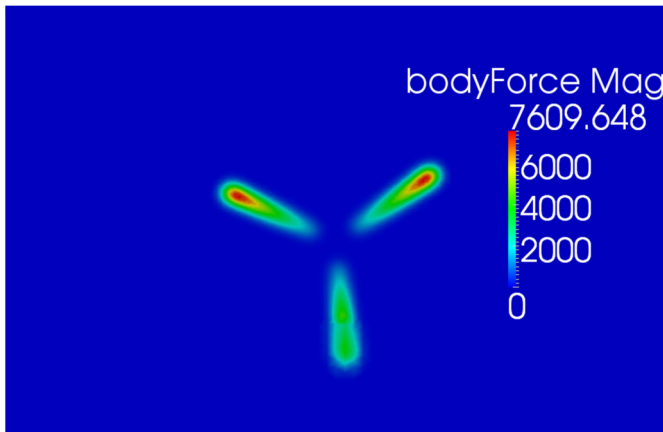


Figure 5-13 Body force distribution at the rotor plane for case 3

The power and thrust graphs are shown in Figure 5-14. From this figure we can see that both the power and the thrust is still too high compared to the reference, however the values are smooth for the different blade angles.

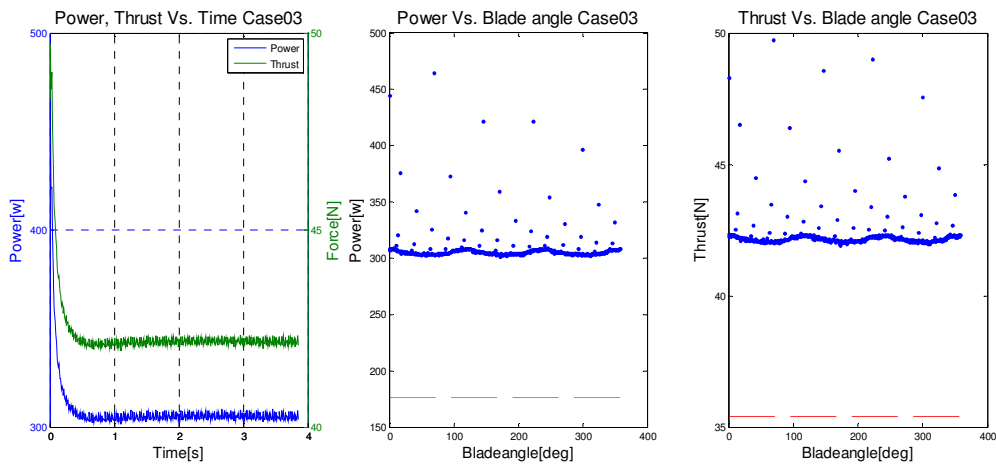


Figure 5-14 Power and thrust graphs for case 3

From Figure 5-15 we can see that the root velocity is still too high, for all the wake profiles.

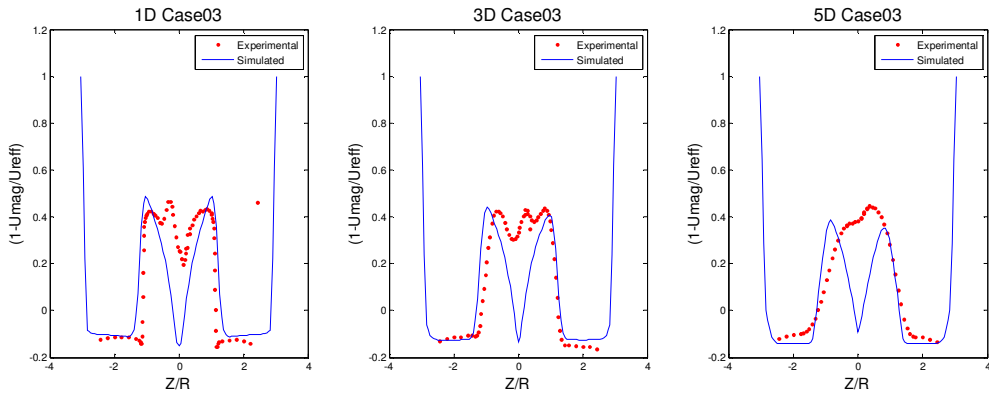


Figure 5-15 Velocity profile in the wake at 1,3 and 5 rotor diameters downstream from the rotor for case 3

5.1.4 Case 4

For this case the main objective was to get a better model hub of the rotor and achieve a more realistic velocity contour in the center, this was achieved by changing the hub radius parameter in the ALM. However, it was later discovered that this approach changes the rotor size, and therefore needed improvement. The case profile is shown in Figure 5-16.

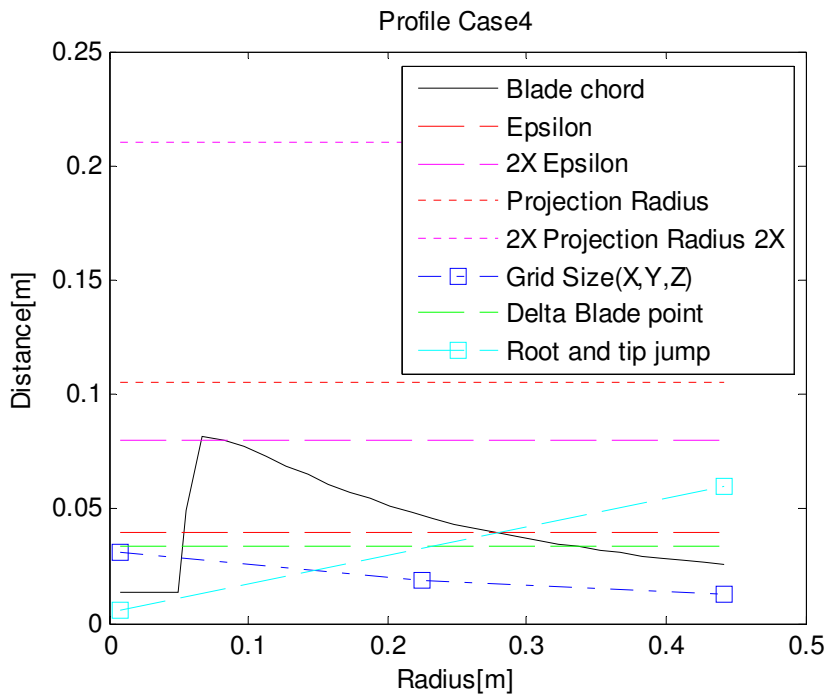


Figure 5-16 Case profile for case 4

In Figure 5-17 we can see the velocity contour. For this case, the center velocity is reduced significantly.

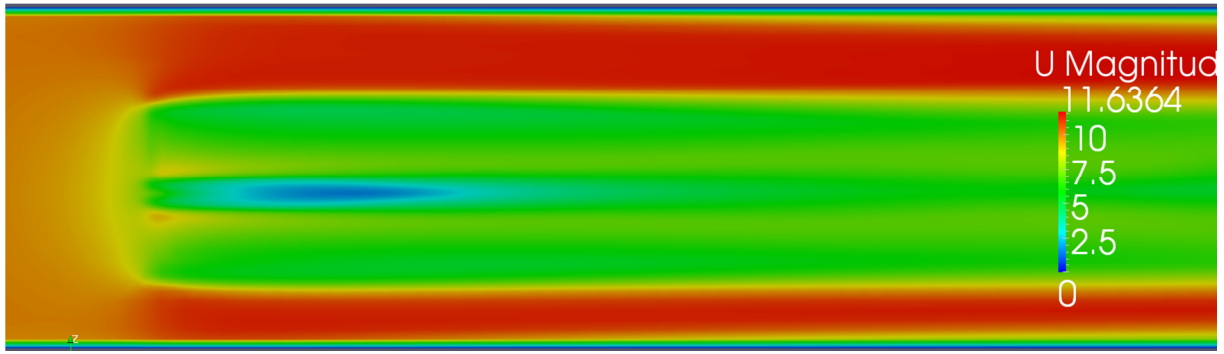


Figure 5-17 Velocity contour in the center plane through the rotor for case 4

From the force distribution shown in Figure 5-18, we can see that there are more forces in the center of the rotor.

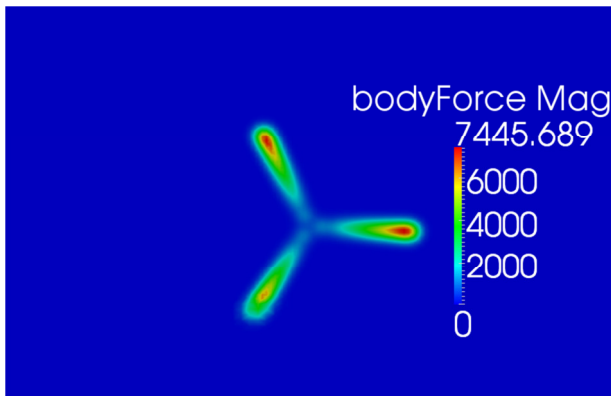


Figure 5-18 Body force distribution at the rotor plane for case 4

The power and thrust calculations which are shown in Figure 5-19 are still too high compared to the reference.

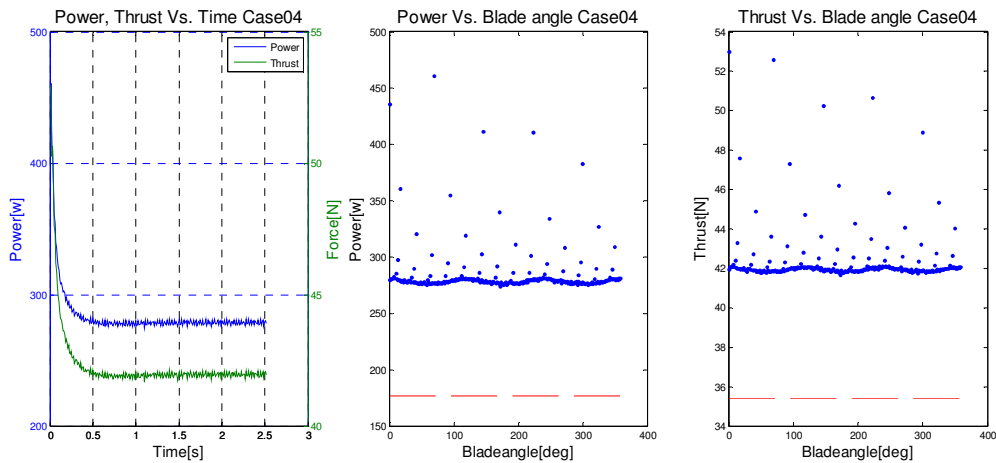


Figure 5-19 Power and thrust graphs for case 4

When we look at the velocity profiles in Figure 5-20, we can see that the center flow for 1 diameter behind the rotor, is slower than the experimental data, for 3 diameters and for 5 diameters the data is a better match with the experiment data, but can still be improved.

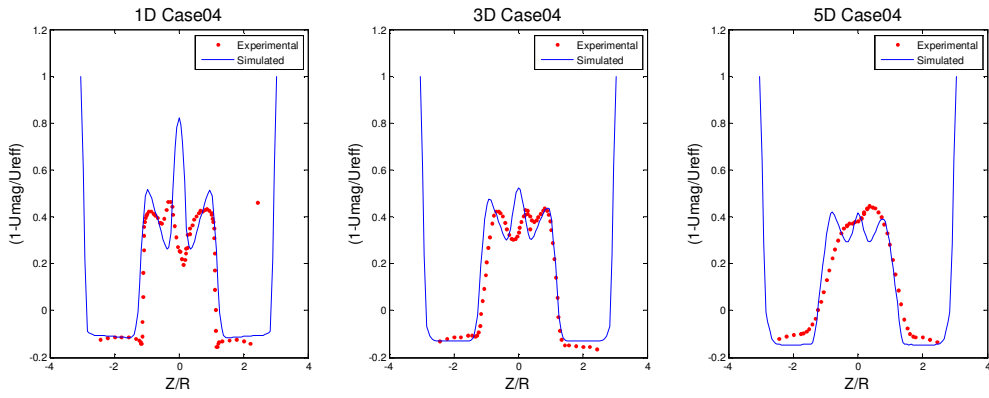


Figure 5-20 Velocity profile in the wake at 1,3 and 5 rotor diameters downstream from the rotor for case 4

5.1.5 Case 5

This case is mostly similar to the previous case, but has some corrections in the grid refinement boundaries.



Figure 5-21 Grid in the center plane for case 5

The mesh is now composed of 2654868 cells, the mesh after refining is shown in Figure 5-21 and the refinement ranges as shown in Table 5-4.

Table 5-4 Grid refinement limits for case 5

	X		Y		Z	
Level 1	-1.0	7.0	-1.3	1.3	0.0	1.8
Level 2	-0.6	6.5	-1.2	1.2	0.1	1.7
Level 3	-0.3	6.0	-1.0	1.0	0.2	1.6

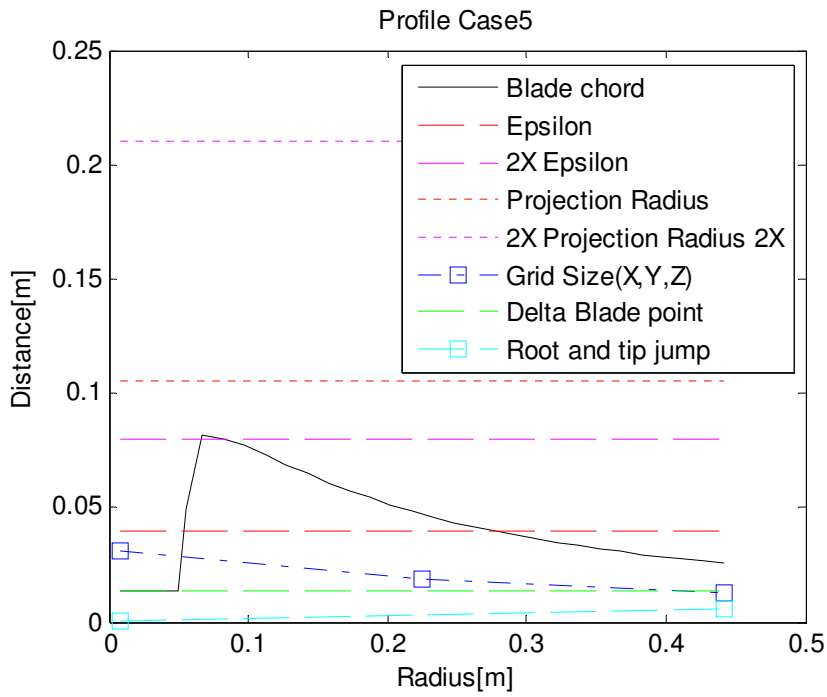


Figure 5-22 Case profile for case 5

In Figure 5-23 we can see the velocity contour. For this case, the center velocity is reduced significantly.

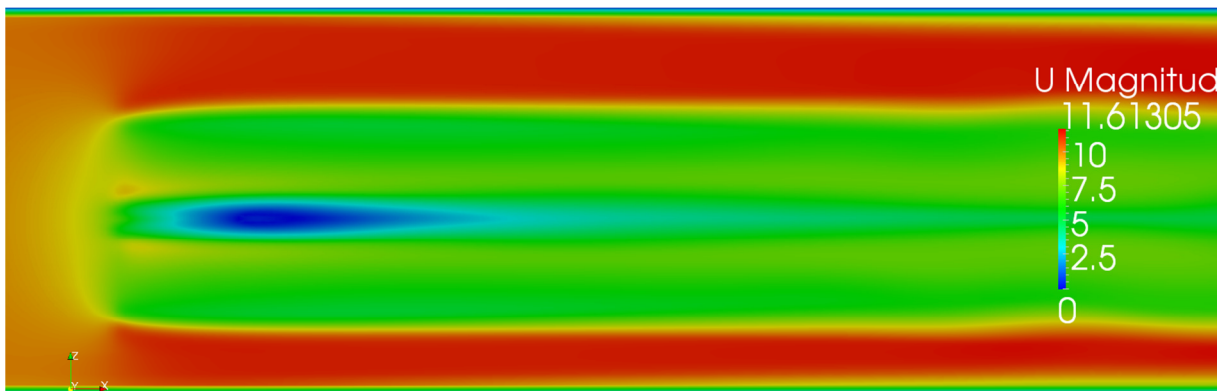


Figure 5-23 Velocity contour in the center plane through the rotor for case 5

From the force distribution shown in Figure 5-24, we can see that there are more forces in the center of the rotor. Also the blades now looks more similar.

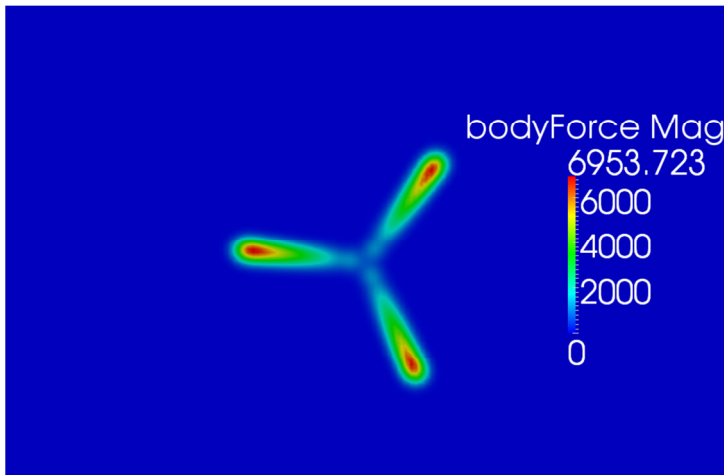


Figure 5-24 Body force distribution at the rotor plane for case 5

The power and thrust calculations which are shown in Figure 5-25 are still too high compared to the reference.

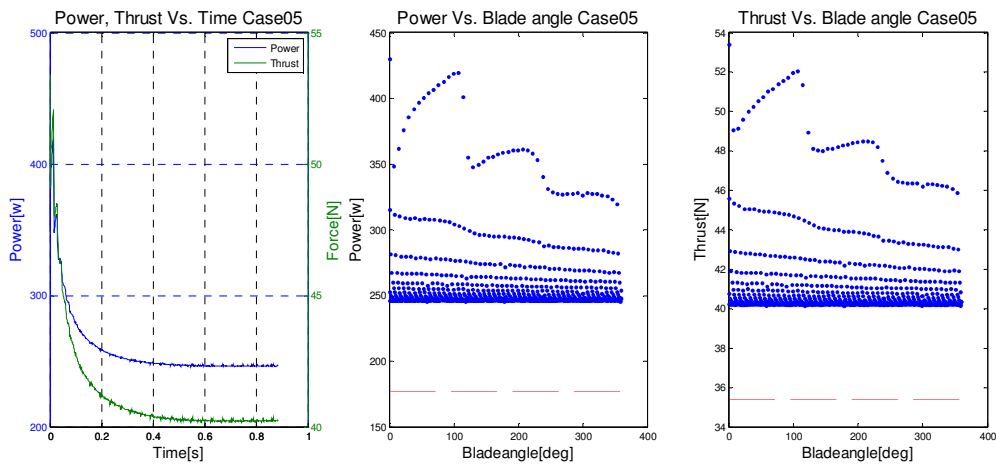


Figure 5-25 Power and thrust graphs for case 5

When we look at the velocity profiles in Figure 5-26, we can see that the center flow for 1 diameter behind the rotor, is slower than the experimental data, for 3 diameters and for 5 diameters the data is a better match with the experiment data, but can still be improved.

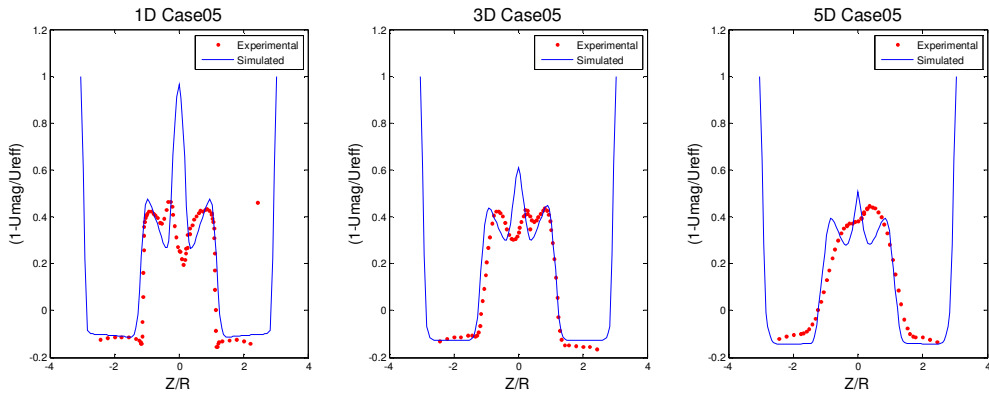


Figure 5-26 Velocity profile in the wake at 1,3 and 5 rotor diameters downstream from the rotor for case 5

5.1.6 Case 6

This case was an extreme test to see the effect of a very small epsilon factor.

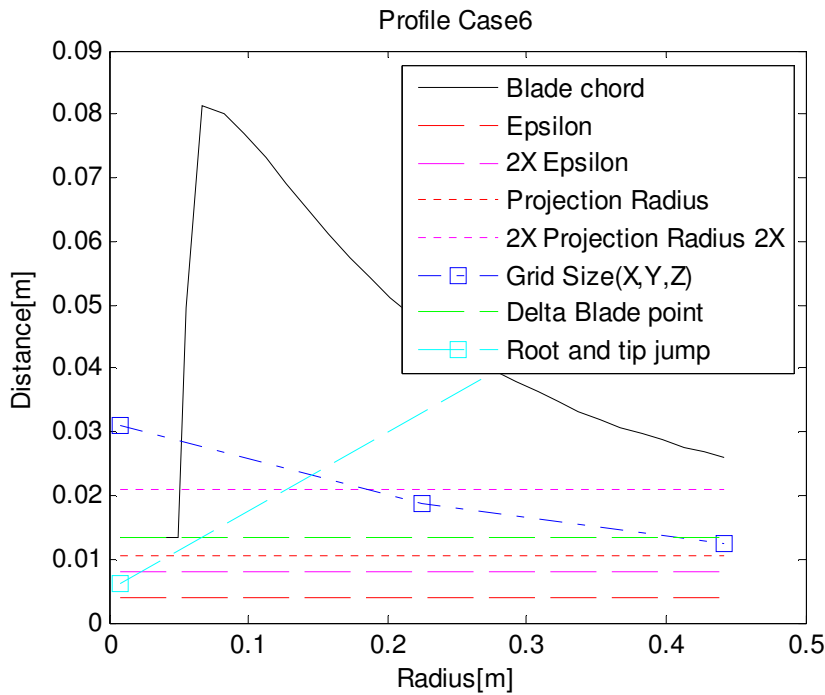


Figure 5-27 Case profile for case 6

This case gives a very bad flow influence, which looks more or less unchanged. The velocity contour is shown in Figure 5-28.



Figure 5-28 Velocity contour in the center plane through the rotor for case 6

With a low epsilon value, the force distribution that are shown in Figure 5-29, looks a bit strange and is not reasonable, all the power is distributed in just a few points.

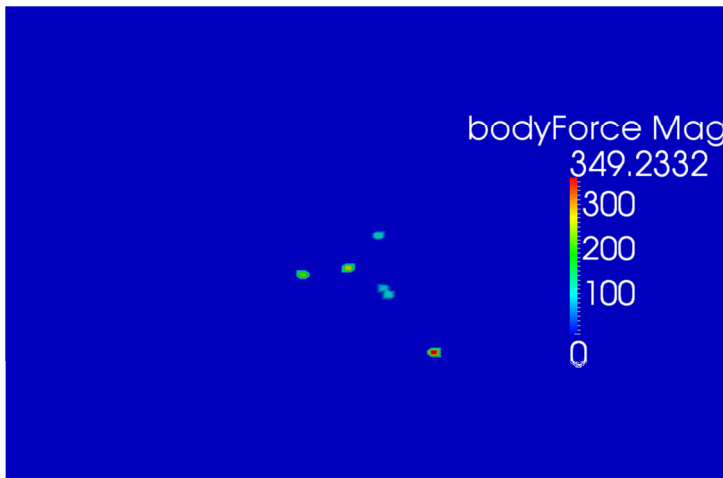


Figure 5-29 Body force distribution at the rotor plane for case 6

The power and thrust calculation are also bad for this case and are far above the reference values. The graphs can be found in Figure 5-30.

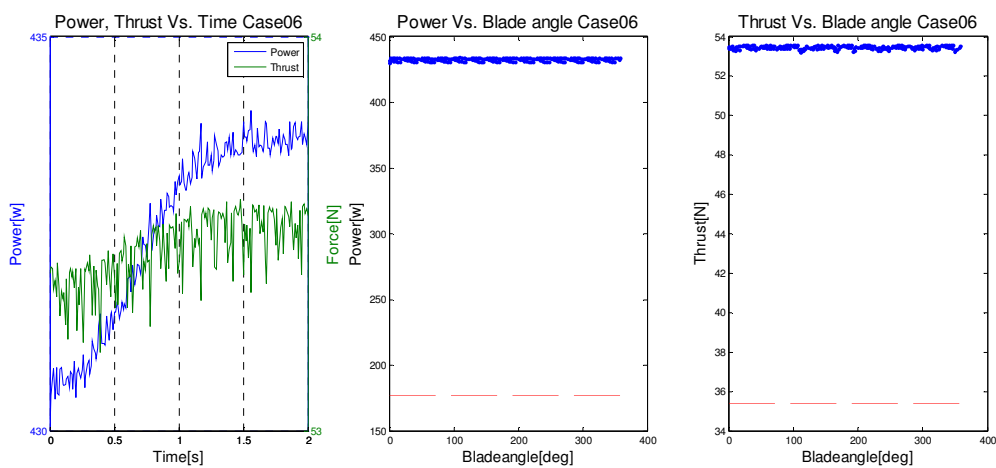


Figure 5-30 Power and thrust graphs for case 6

The velocity profiles shown in Figure 5-31 are far from the experimental data.

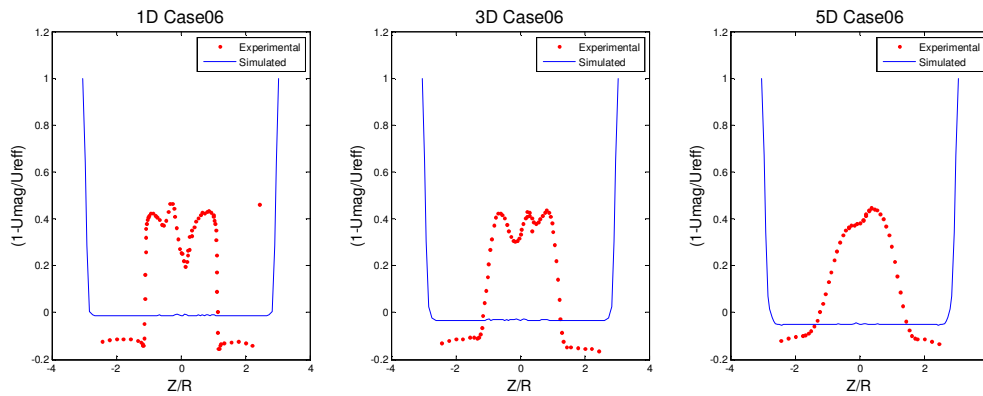


Figure 5-31 Velocity profile in the wake at 1,3 and 5 rotor diameters downstream from the rotor for case 6

5.1.7 Case 7

This case uses the Glauert root and tip correction. This is an option in the ALM, and it might reduce the calculated power. In addition, the size of the grid refinement was reduced to speed up the simulation. The mesh ended up with 178836 cells, so a good reduction. The refinement limits are shown in Table 5-5.

Table 5-5 Grid refinement limits for case 7

	X		Y		Z	
Level 1	-1.2	7.0	-1.3	1.3	0.0	1.8
Level 2	-0.7	2.5	-1.2	1.2	0.0	1.8
Level 3	-0.4	0.7	-1.0	1.0	0.0	1.8

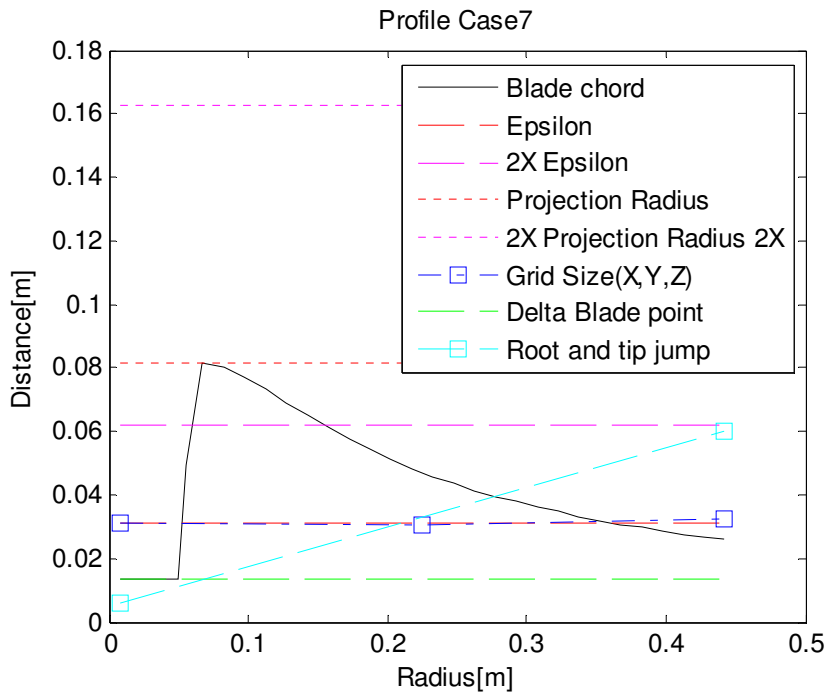


Figure 5-32 Case profile for case 7

In Figure 5-23 we can see the velocity contour. For this case, the center velocity is reduced significantly.

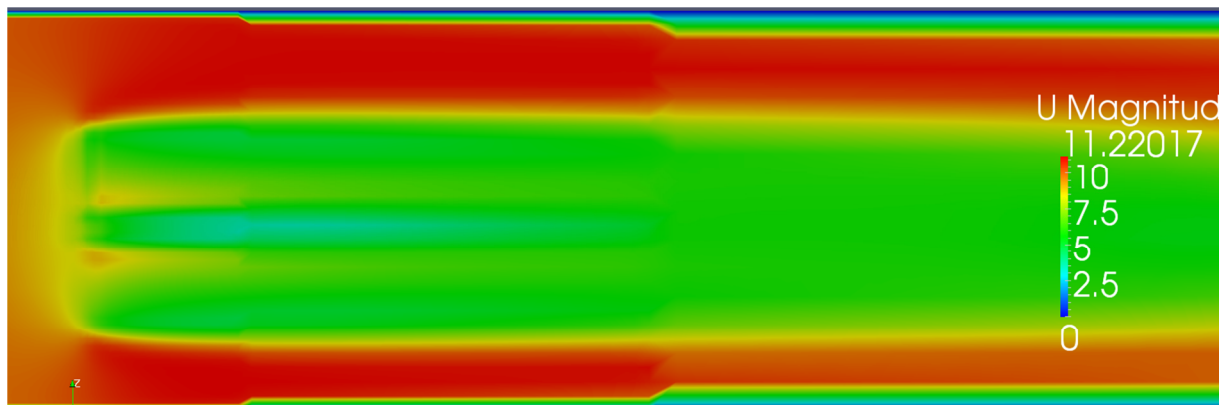


Figure 5-33 Velocity contour in the center plane through the rotor for case 7

From the force distribution shown in Figure 5-24, we can see that there are more forces in the center of the rotor. In addition, the blades have equal loading.

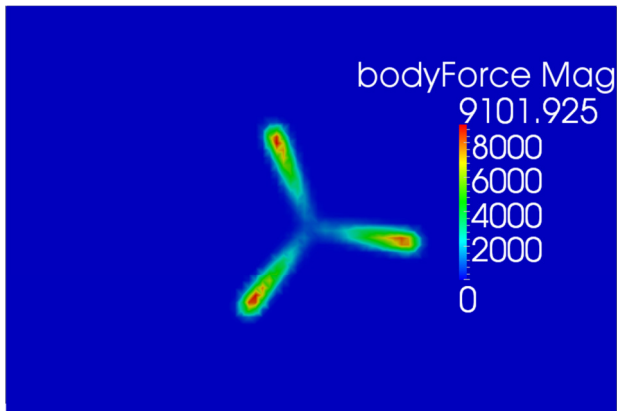


Figure 5-34 Body force distribution at the rotor plane for case 7

The power and thrust calculations which are shown in Figure 5-35 are still too high compared to the reference. The data are a bit noisy, which is caused by the discretization process combined with a small time step.

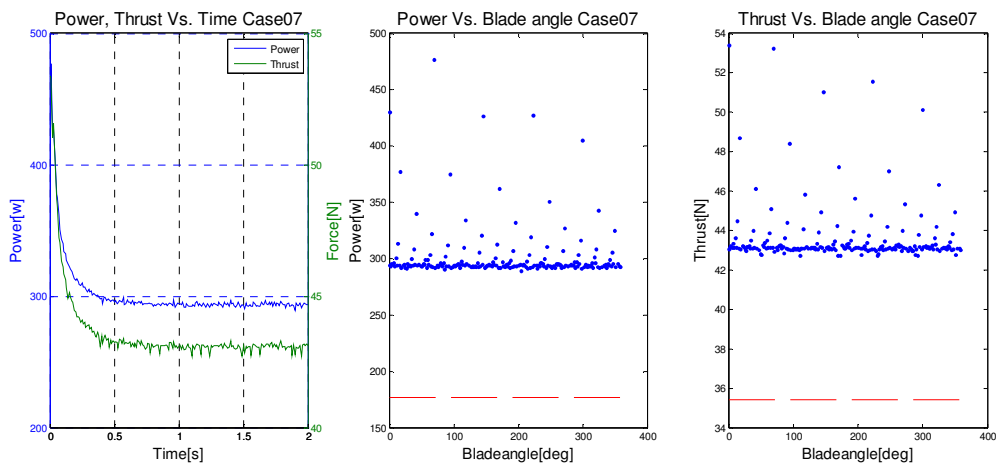


Figure 5-35 Power and thrust graphs for case 7

The velocity profile shown in Figure 5-36 are very close to the experimental data.

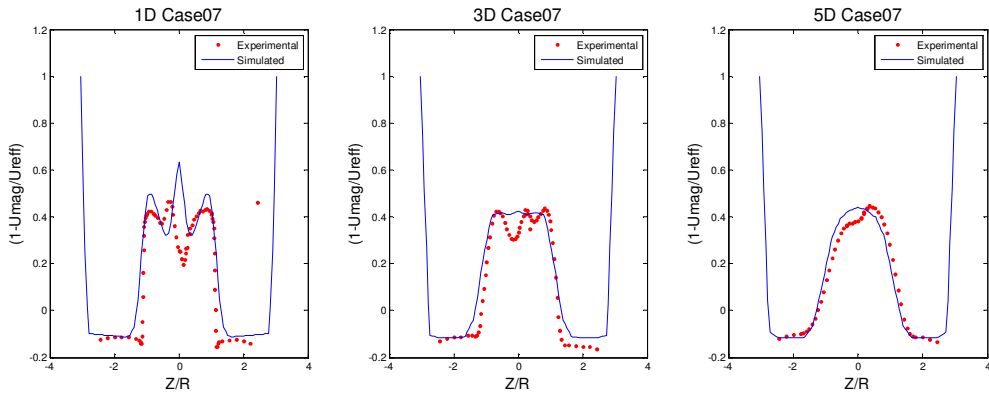


Figure 5-36 Velocity profile in the wake at 1,3 and 5 rotor diameters downstream from the rotor for case 7

5.1.8 Case 8

This case has a major change in grid structure and grid refinement boundaries

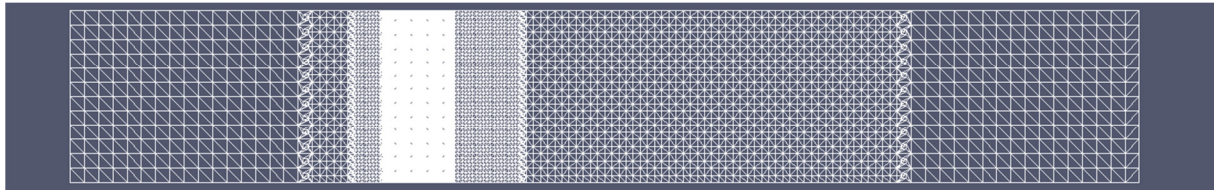


Figure 5-37 Grid in the center plane for case 8

The mesh for this case is found in Figure 5-37 and is consisting of 676944 cells, the refinement limits are shown in Table 5-6.

Table 5-6 Grid refinement limits for case 8

	X		Y		Z	
Level 1	-1.2	5.0	-1.355	1.355	0.0	1.8
Level 2	-0.7	1.0	-1.355	1.355	0.0	1.8
Level 3	-0.4	0.3	-1.355	1.355	0.0	1.8

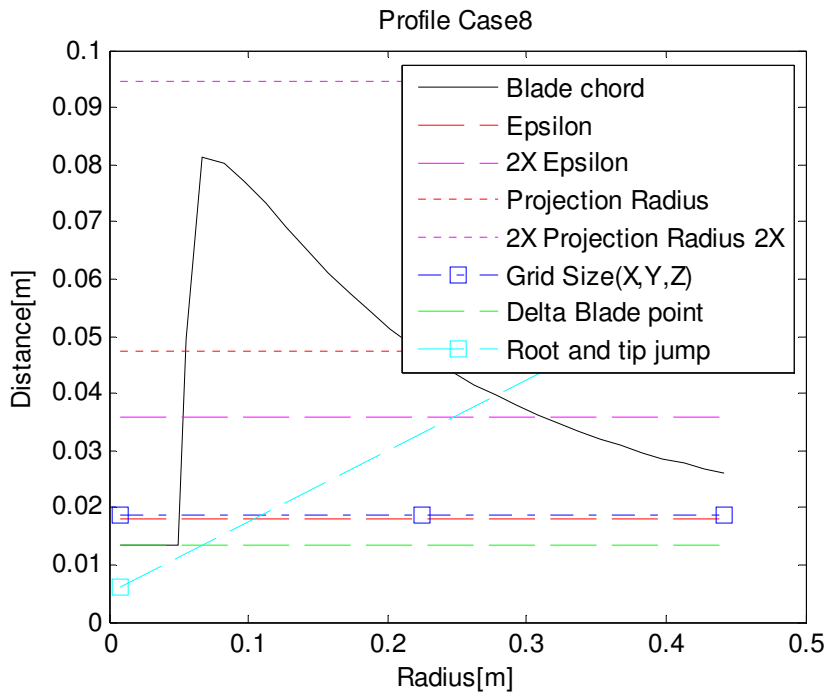


Figure 5-38 Case profile for case 8

In Figure 5-39 we can see the velocity contour. For this case, the center velocity is reduced significantly.

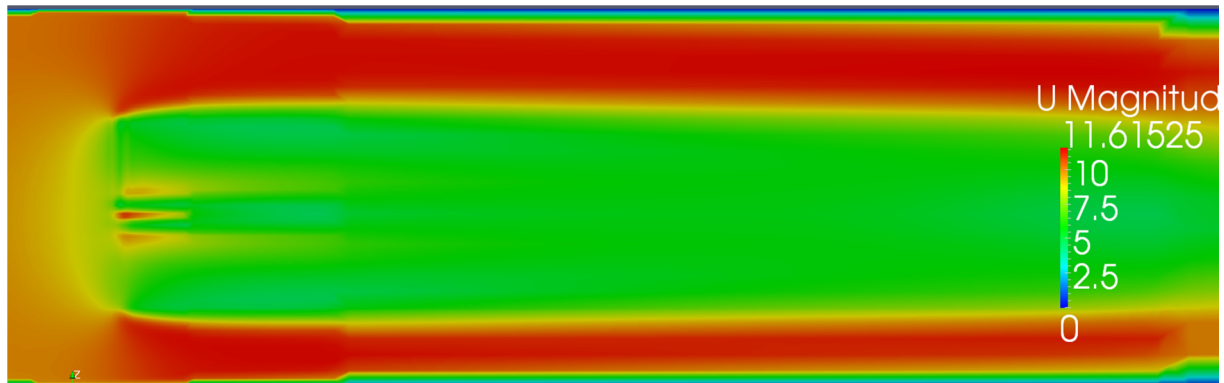


Figure 5-39 Velocity contour in the center plane through the rotor for case 8

From the force distribution shown in Figure 5-40 we can see that the blades are narrower than earlier.

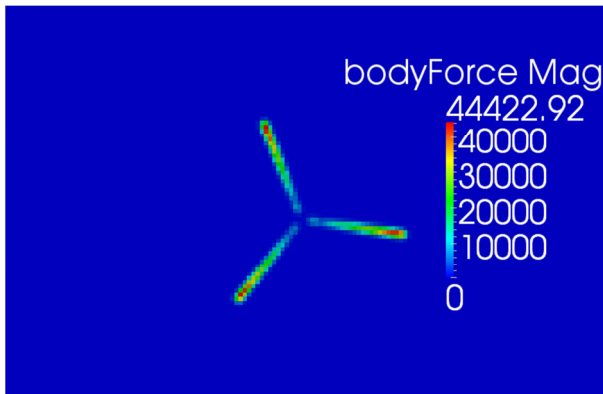


Figure 5-40 Body force distribution at the rotor plane for case 8

The power and thrust calculations which are shown in Figure 5-41 are still too high compared to the reference. The data are a bit noisy, which is caused by the discretization process combined with a small time step.

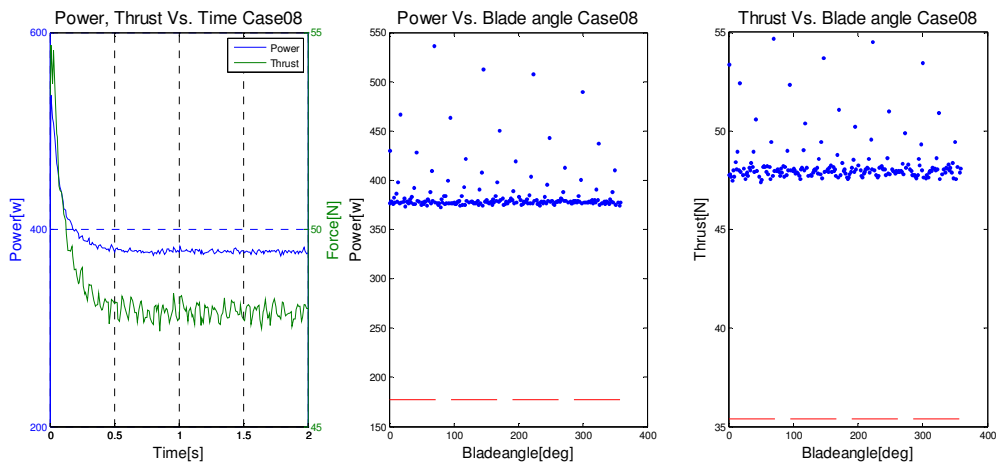


Figure 5-41 Power and thrust graphs for case 8

The velocity profile shown in Figure 5-42 are very close to the experimental data.

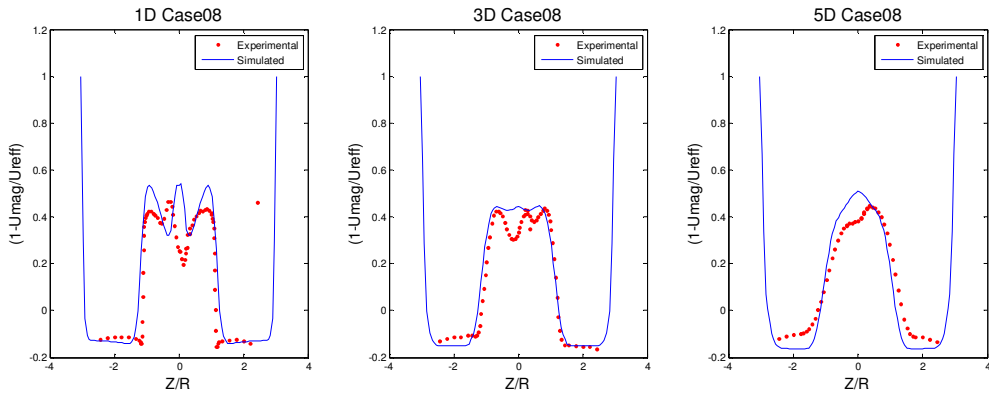


Figure 5-42 Velocity profile in the wake at 1,3 and 5 rotor diameters downstream from the rotor for case 8

5.1.9 Case 9

In order to achieve the hub effect of the flow without altering the rotor dimensions, the hub was modeled as a separate turbine in this case. The new turbine is supposed to give the same effect as earlier cases, but not change the rotor size and not load the rotor and changing the power calculations. The separate turbine is modeled as cylinders with just drag and no lift forces.

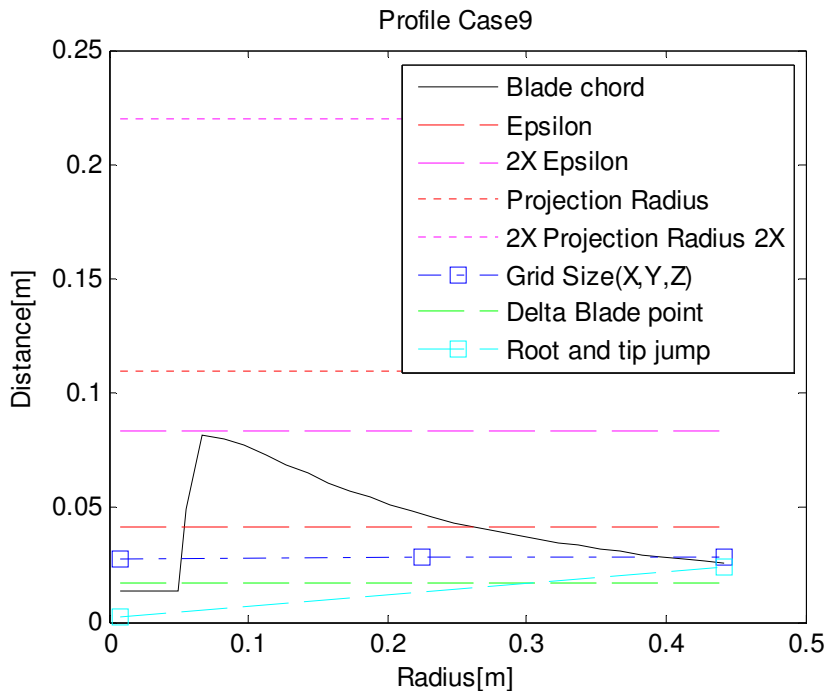


Figure 5-43 Case profile for case 9

The power and thrust calculations which are shown in Figure 5-44 are still too high compared to the reference.

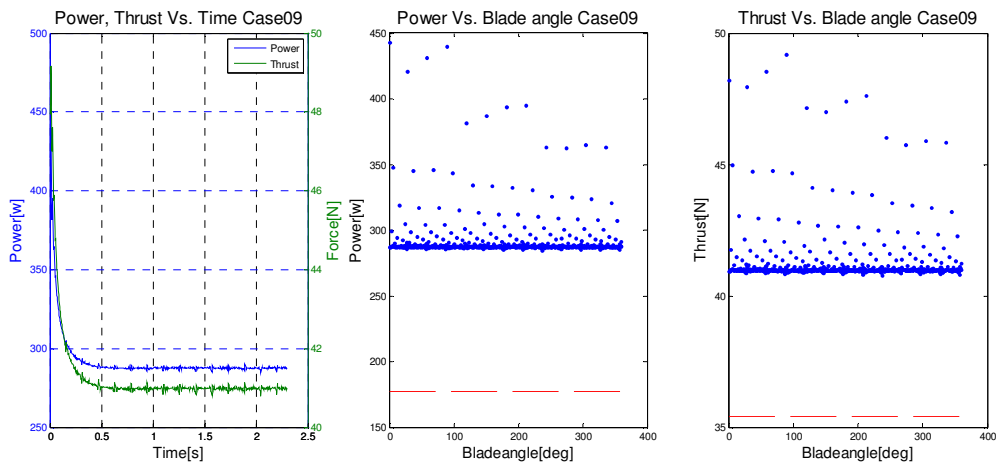


Figure 5-44 Power and thrust graphs for case 9

The velocity profiles shown in Figure 5-45 are close to the experimental data, but could be improved.

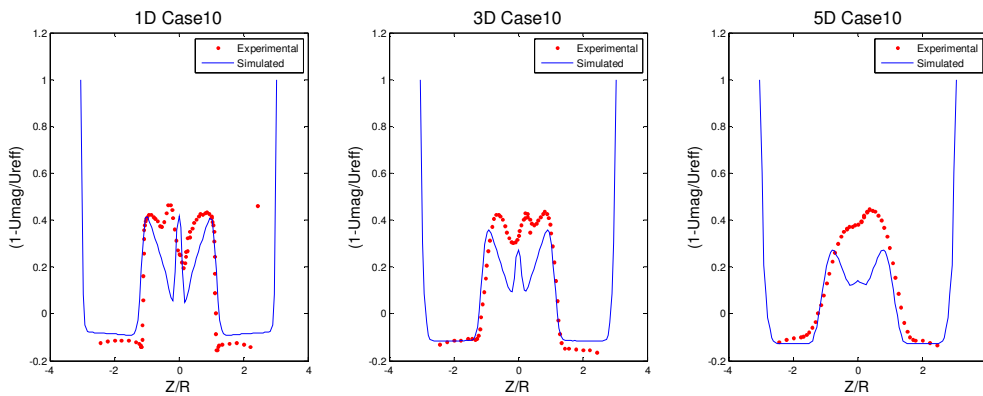


Figure 5-45 Velocity profile in the wake at 1,3 and 5 rotor diameters downstream from the rotor for case 9

5.1.10 Case 10

The difference from last case is the time step and the mesh.

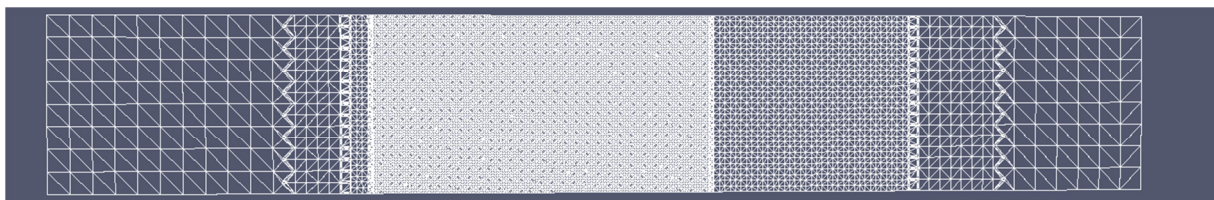


Figure 5-46 Grid in the center plane for case 10

The mesh which is shown in Figure 5-46 is consisting of 819264 cells, the refinement limits can be found in Table 5-7.

Table 5-7 Grid refinement limits for case 10

	X		Y		Z	
Level 1	-1.2	6.0	-1.355	1.355	0.0	1.8
Level 2	-0.7	5.0	-1.355	1.355	0.0	1.8
Level 3	-0.4	3.0	-1.355	1.355	0.0	1.8

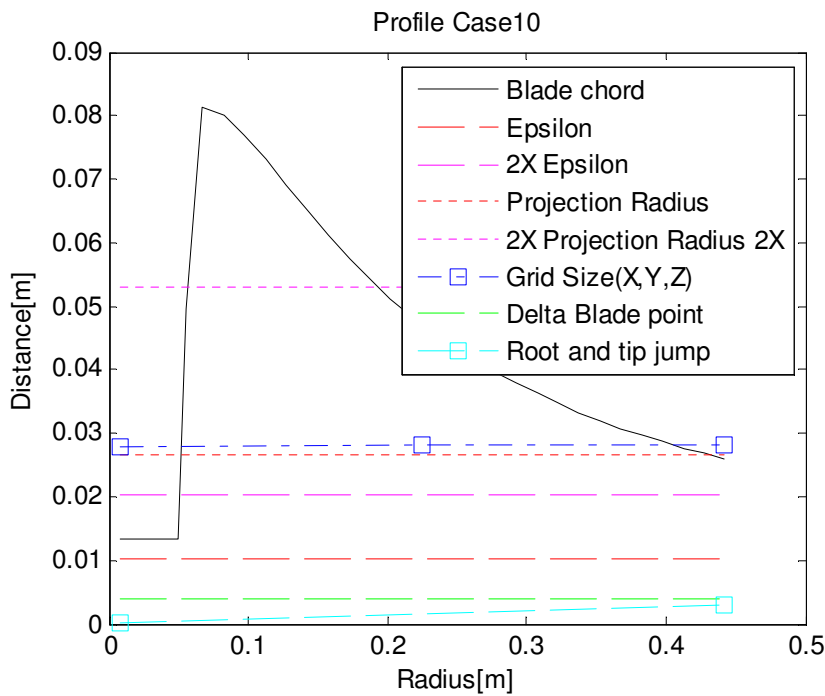


Figure 5-47 Case profile for case 10

In Figure 5-39 we can see the velocity contour. Here we can see the influence from the hub model in the center of the flow.

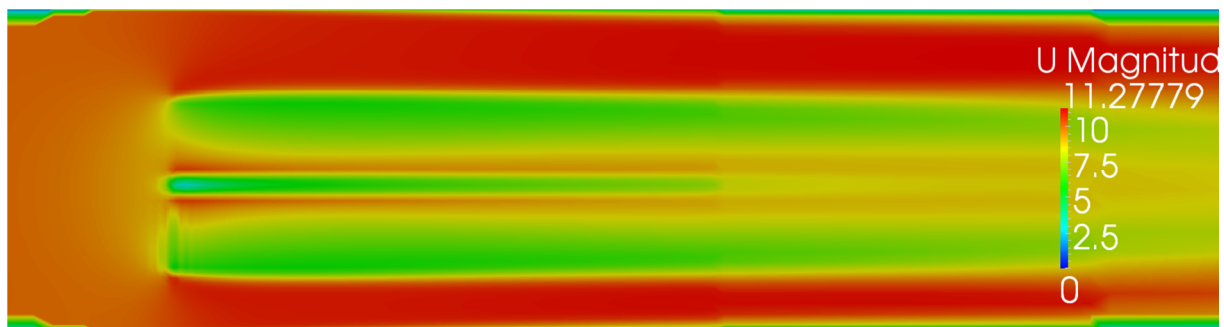


Figure 5-48 Velocity contour in the center plane through the rotor for case 10

From the force distribution shown in Figure 5-49 we can see that the blades are narrower than earlier, almost just a row of single cells. This is due to the low epsilon value.

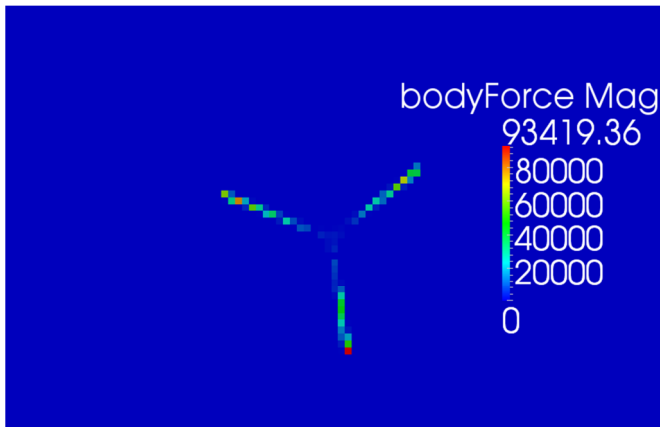


Figure 5-49 Body force distribution at the rotor plane for case 10

The power and thrust calculations which are shown in Figure 5-35 quite good compared to the reference. However the data is very noisy, which is caused by the discretization process combined with a small time step, and also a small epsilon value.

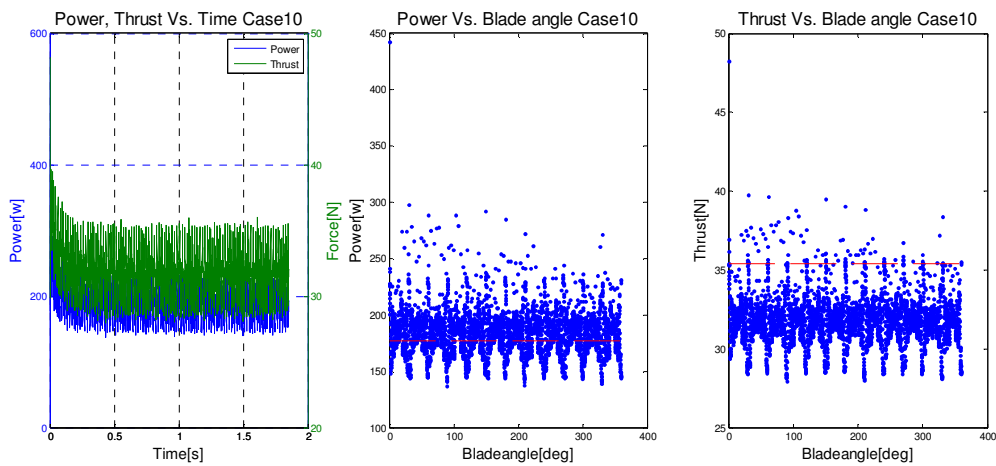


Figure 5-50 Power and thrust graphs for case 10

The velocity profiles shown in Figure 5-51 are close to the experimental data, but could be improved.

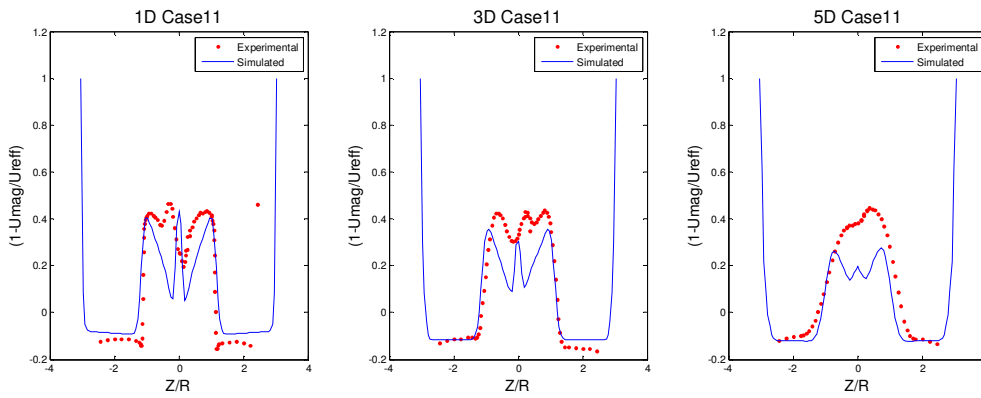


Figure 5-51 Velocity profile in the wake at 1,3 and 5 rotor diameters downstream from the rotor for case 10

5.1.11 Case 11

In an attempt to get a better match on the asymmetry in the velocity profile, a model for the tower was added. It was implemented similarly as the hub model, but just one blade and zero rotation speed.

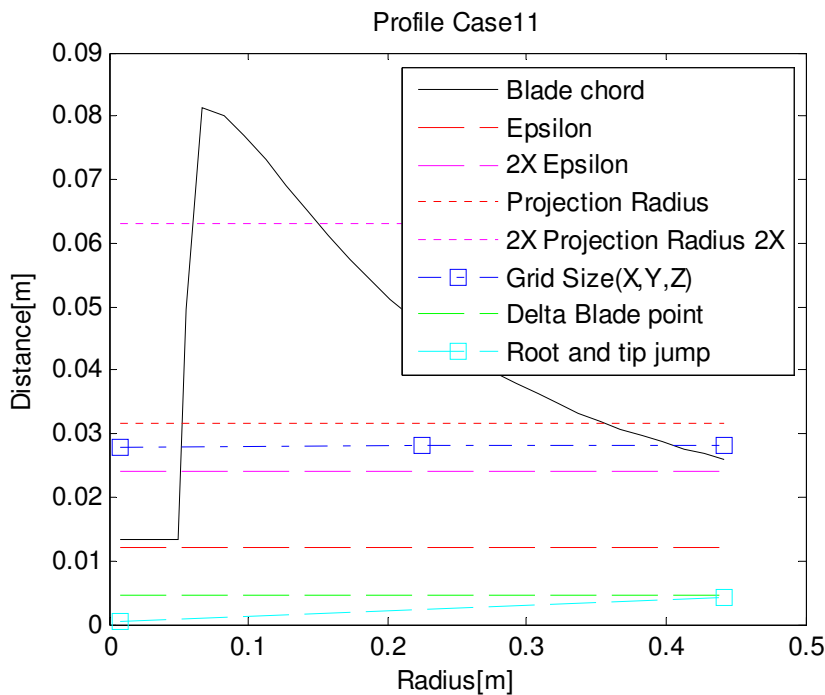


Figure 5-52 Case profile for case 11

From the velocity contour in Figure 5-53 we can see the influence from the tower model in the flow.

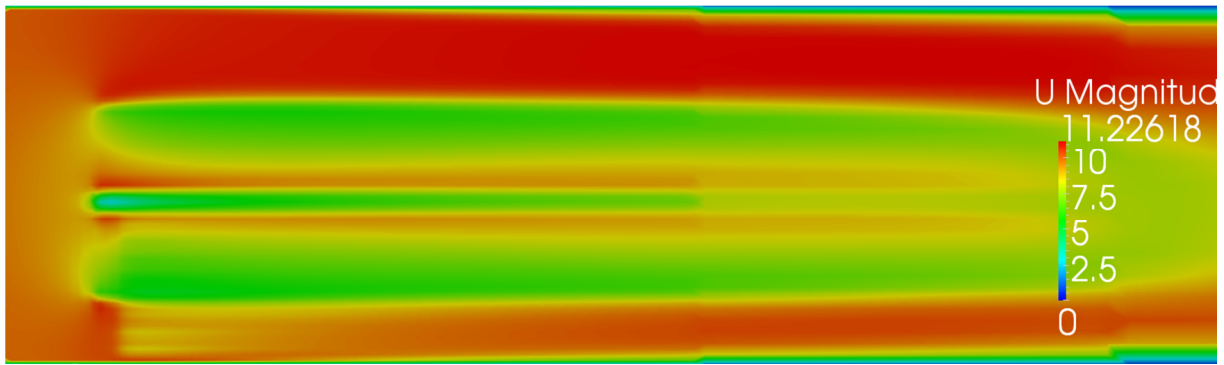


Figure 5-53 Velocity contour in the center plane through the rotor for case 11

From the force distribution shown in Figure 5-54 we can see that the blades are narrow, almost just a row of single cells. This is due to the low epsilon value.

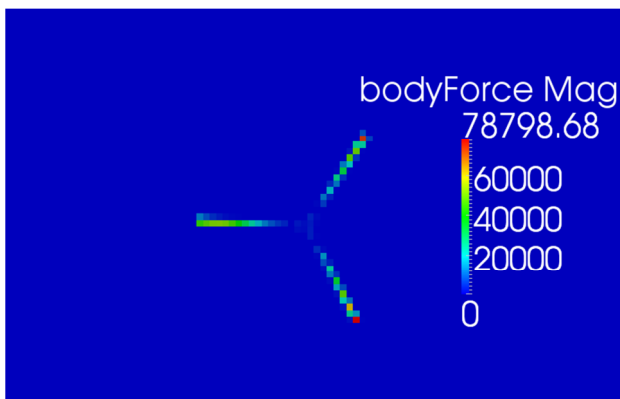


Figure 5-54 Body force distribution at the rotor plane for case 11

The power and thrust calculations which are shown in Figure 5-55 quite good compared to the reference. However, the data is very noisy, which is caused by the discretization process combined with a small time step, and also a small epsilon value.

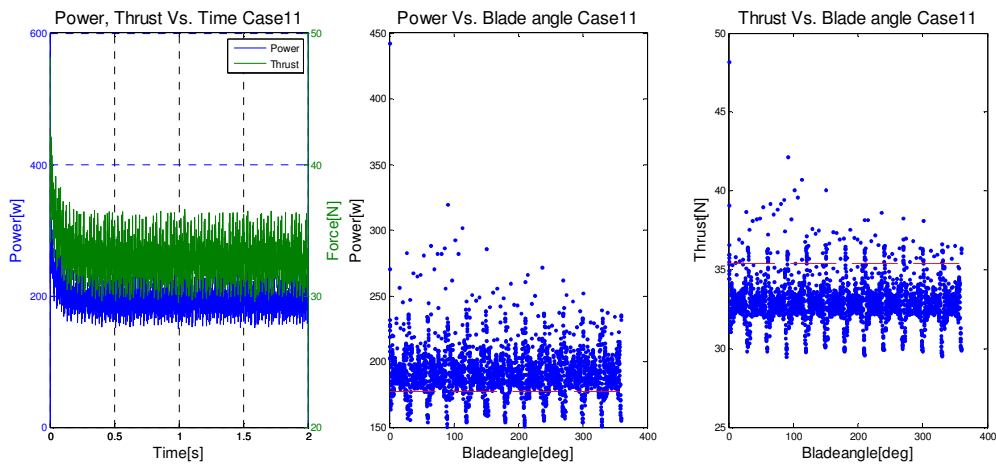


Figure 5-55 Power and thrust graphs for case 11

The velocity profiles shown in Figure 5-56 are close to the experimental data, but could be improved.

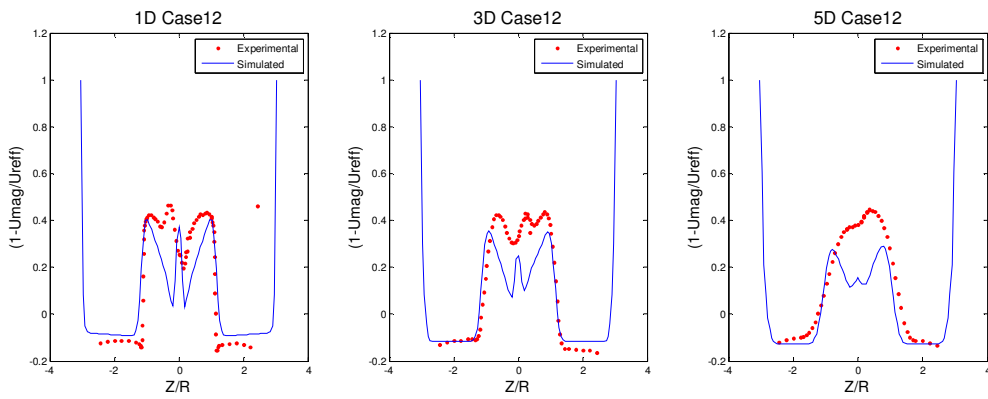


Figure 5-56 Velocity profile in the wake at 1,3 and 5 rotor diameters downstream from the rotor for case 11

5.1.12 Case 12

In order to improve the hub en tower effect the parameter for this models were altered

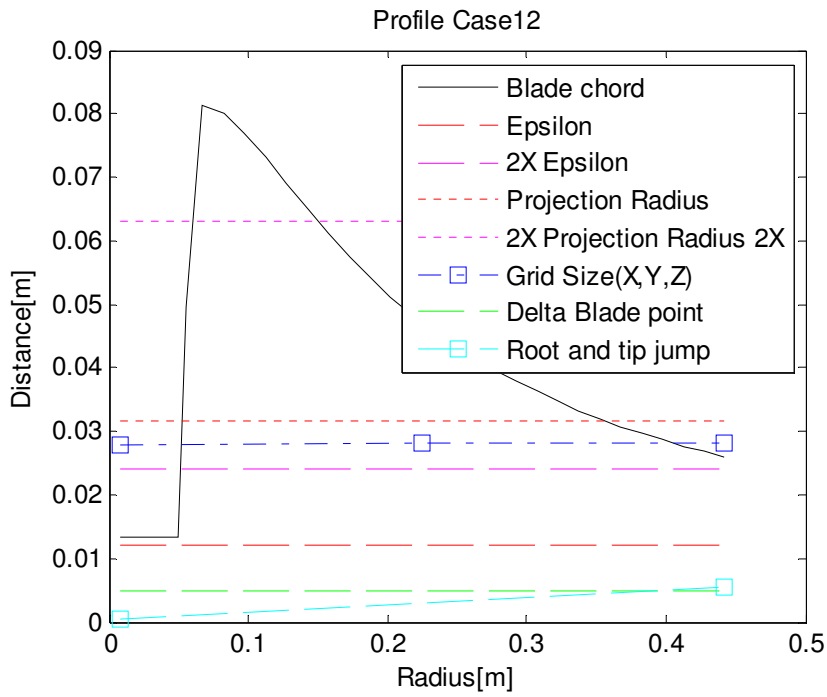


Figure 5-57 Case profile for case 12

From the velocity contour in Figure 5-53 we can see the influence from the tower model in the flow.

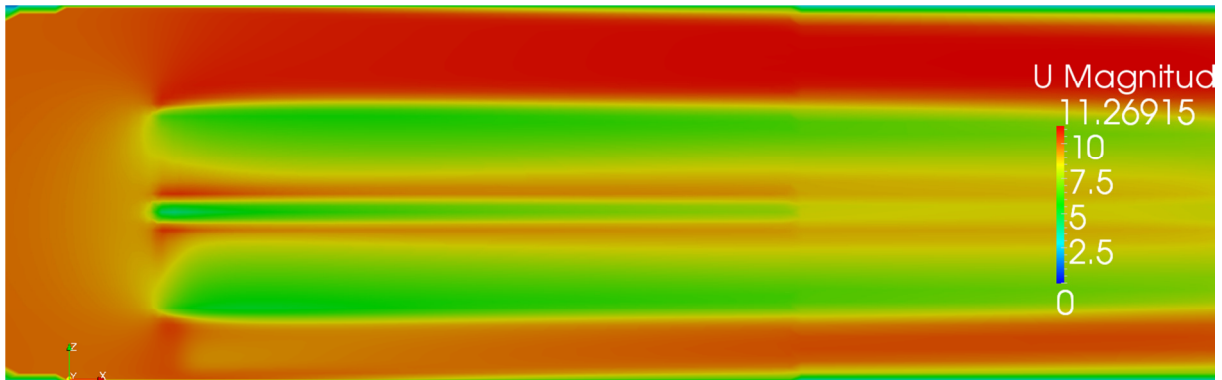


Figure 5-58 Velocity contour in the center plane through the rotor for case 12

From the force distribution shown in Figure 5-59 we can see that the blades are loaded unevenly, this is due to the small time step.

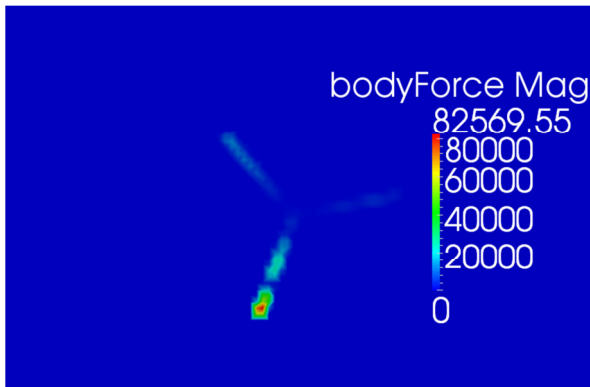


Figure 5-59 Body force distribution at the rotor plane for case 12

The power and thrust calculations which are shown in Figure 5-35 is too low compared to the reference, and is also reporting negative power values. The data is very noisy, which is caused by the discretization process combined with a small time step, and also a small epsilon value.

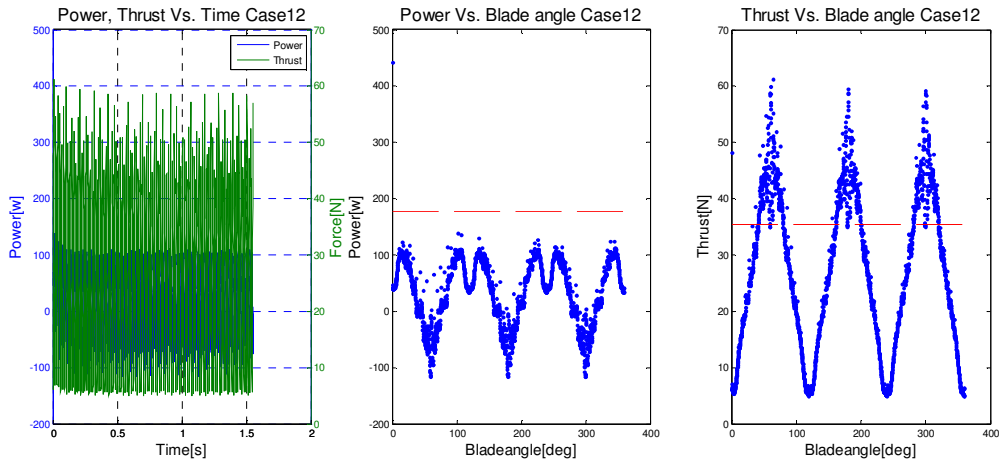


Figure 5-60 Power and thrust graphs for case 12

5.1.13 Case 13

For this case, the implicit solver was used. All parameters are the same as case 12.

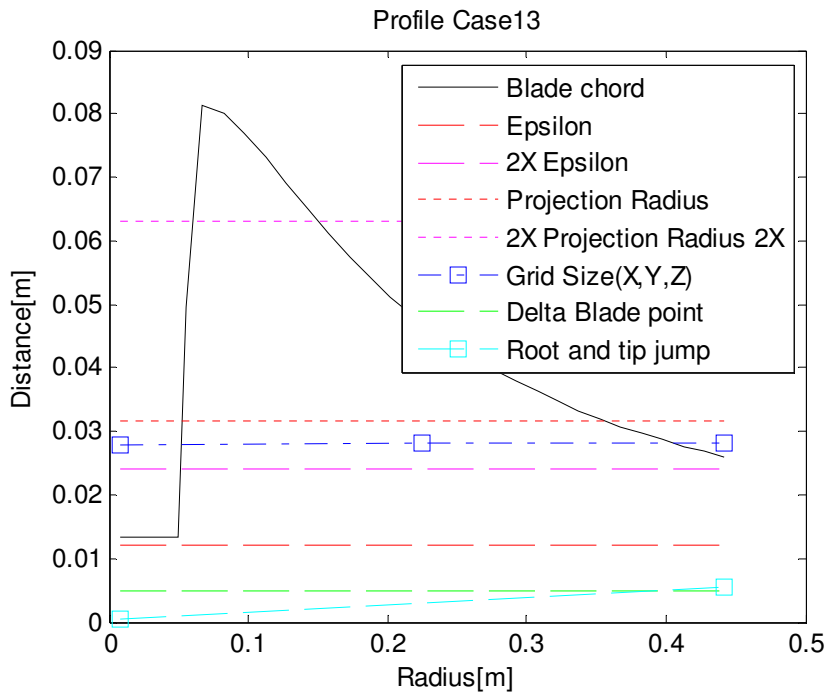


Figure 5-61 Case profile for case 13

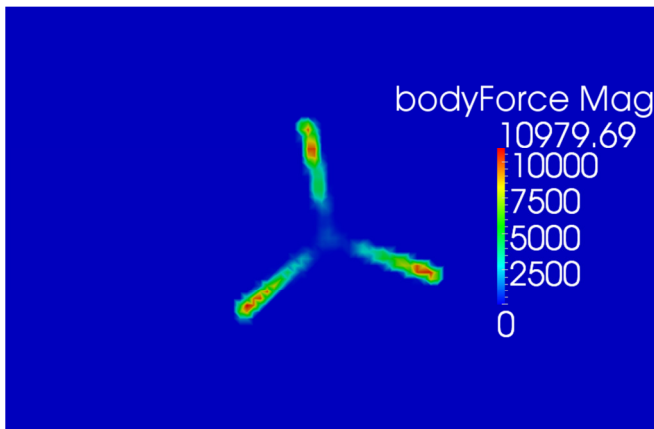


Figure 5-62 Body force distribution at the rotor plane for case 13

The power and thrust calculations which are shown in Figure 5-63 are a bit too low compared to the reference. However, the data is a bit noisy, which is caused by the discretization process combined with a small time step, and also a small epsilon value. The data is less disturbed than the data from case 12, which is promising for the implicit solver scheme.

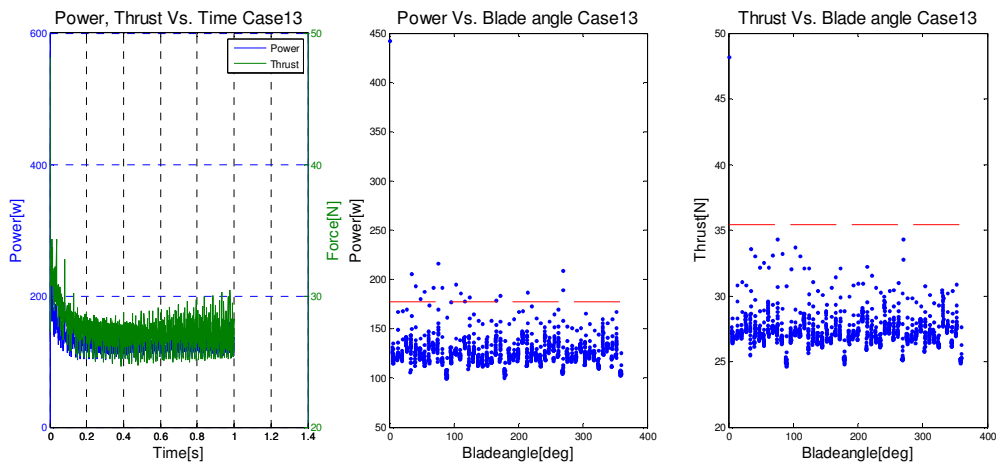


Figure 5-63 Power and thrust graphs for case 13

5.1.14 Case 14

The difference from previous case is just the epsilon factor

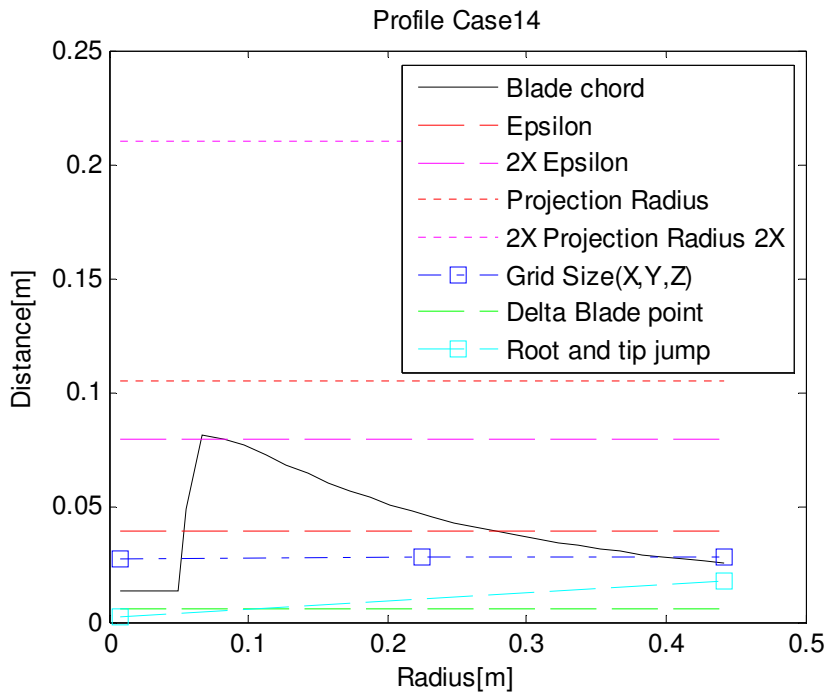


Figure 5-64 Case profile for case 14

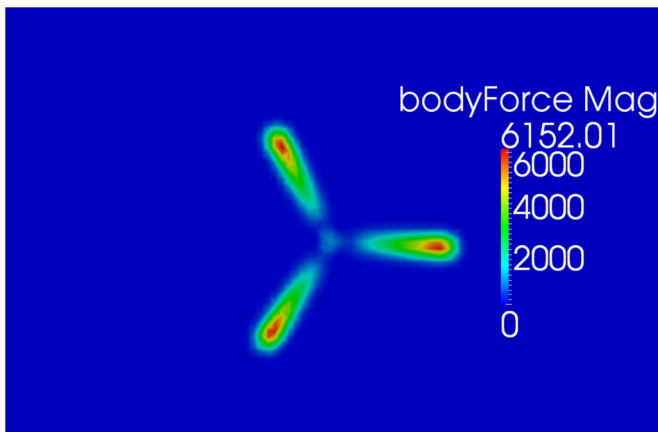


Figure 5-65 Body force distribution at the rotor plane for case 14

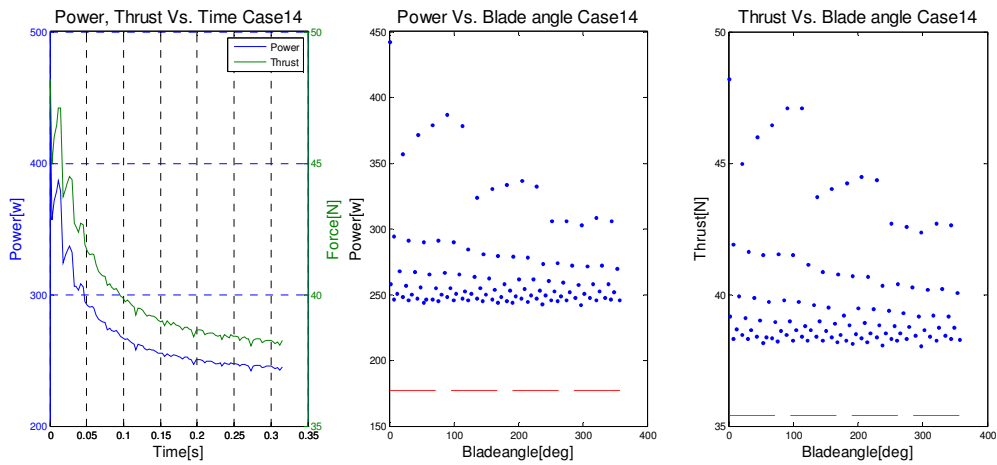


Figure 5-66 Power and thrust graphs for case 14

5.1.15 Case 15

The difference from previous case is just the epsilon factor

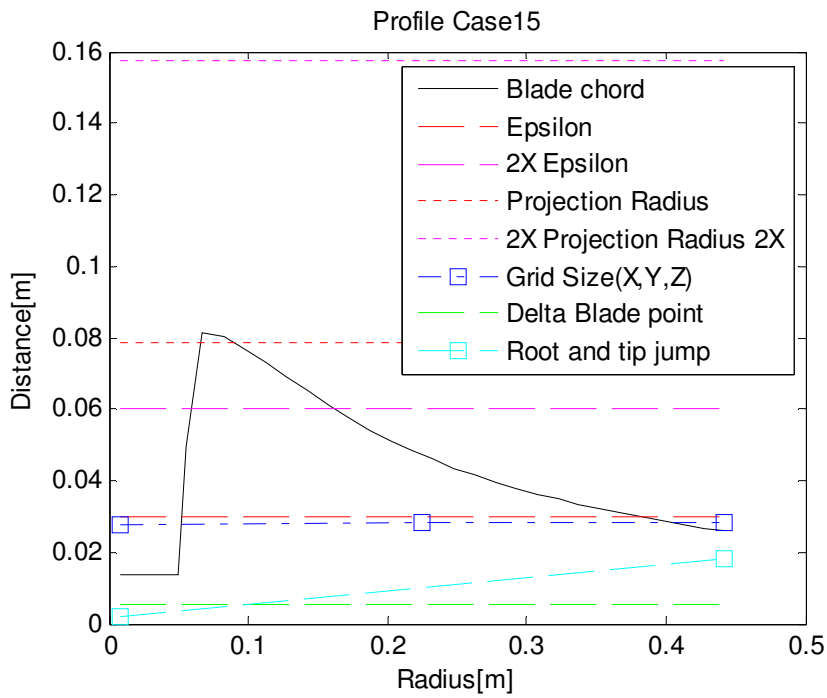


Figure 5-67 Case profile for case 15

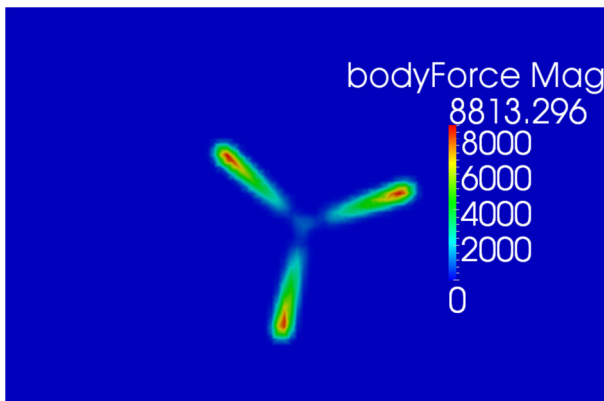


Figure 5-68 Body force distribution at the rotor plane for case 15

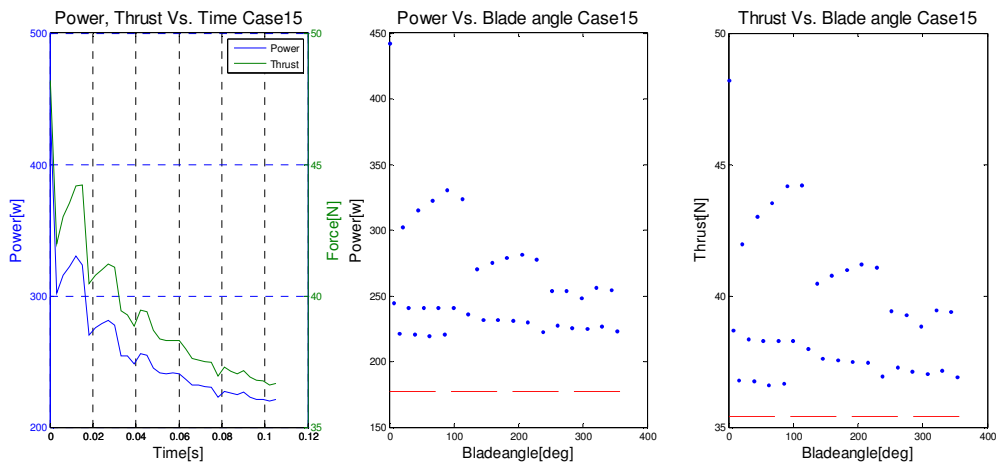


Figure 5-69 Power and thrust graphs for case 15

5.1.16 Case 16

The difference from previous case is just the epsilon factor

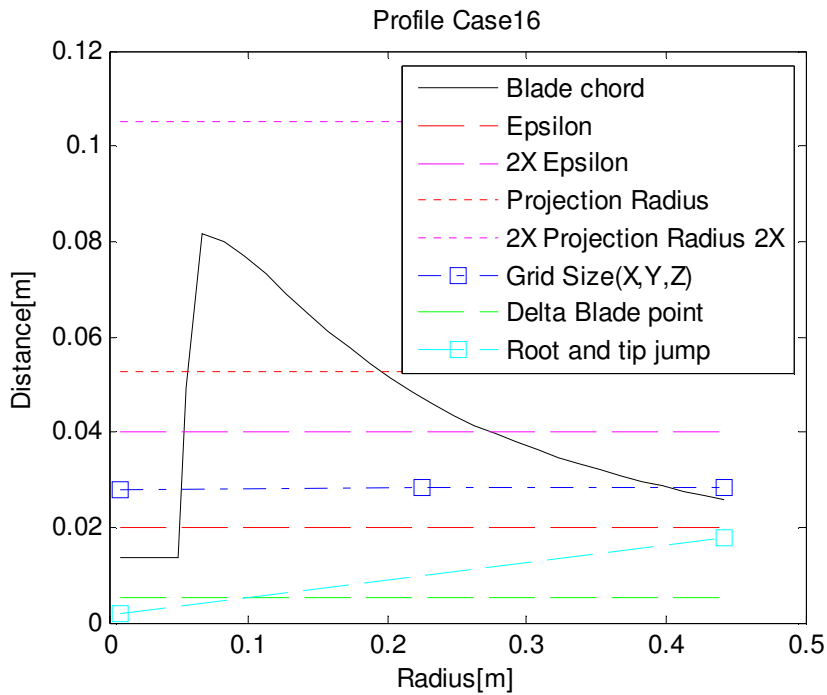


Figure 5-70 Case profile for case 16

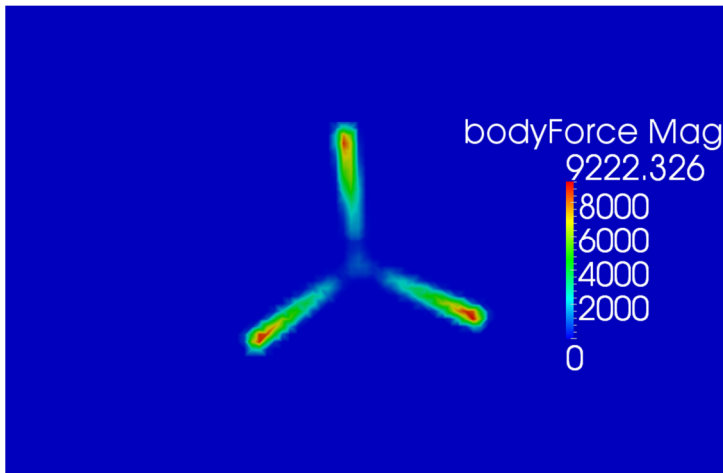


Figure 5-71 Body force distribution at the rotor plane for case 16

The power and thrust calculations which are shown in Figure 5-72 are a bit too low compared to the reference.

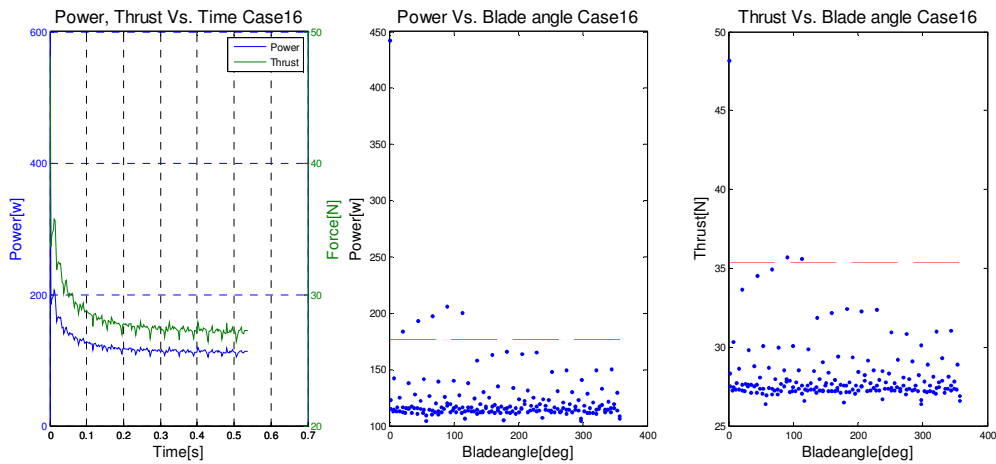


Figure 5-72 Power and thrust graphs for case 16

5.1.17 Case 17

The difference from previous case is just the epsilon factor

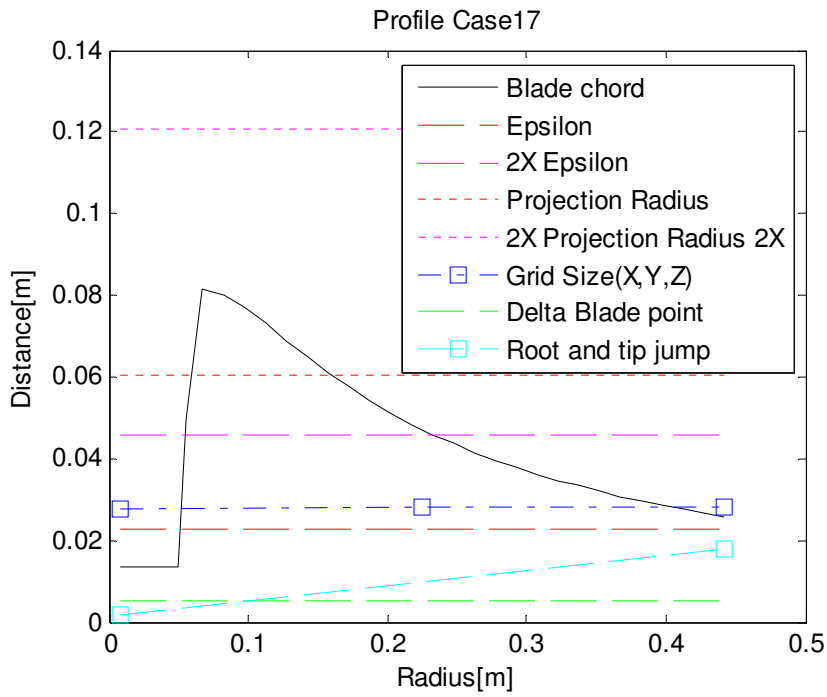


Figure 5-73 Case profile for case 17

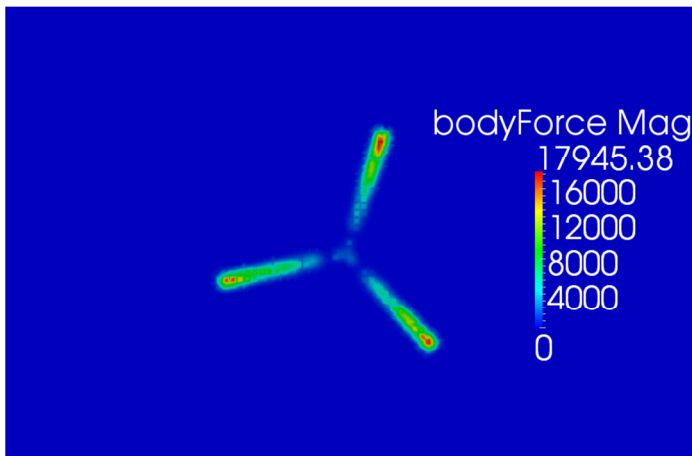


Figure 5-74 Body force distribution at the rotor plane for case 17

The power and thrust calculations which are shown in Figure 5-72 are a bit too low compared to the reference.

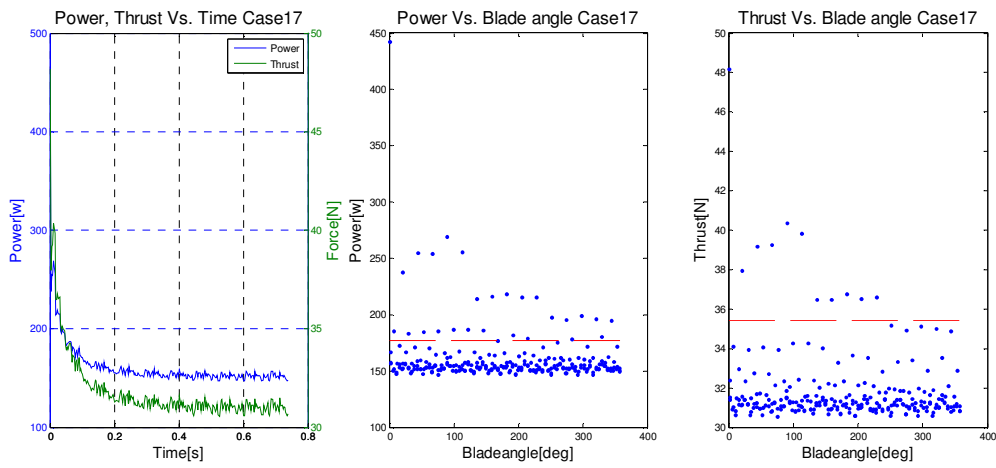


Figure 5-75 Power and thrust graphs for case 17

5.1.18 Case 18

The difference from previous case is just the epsilon factor

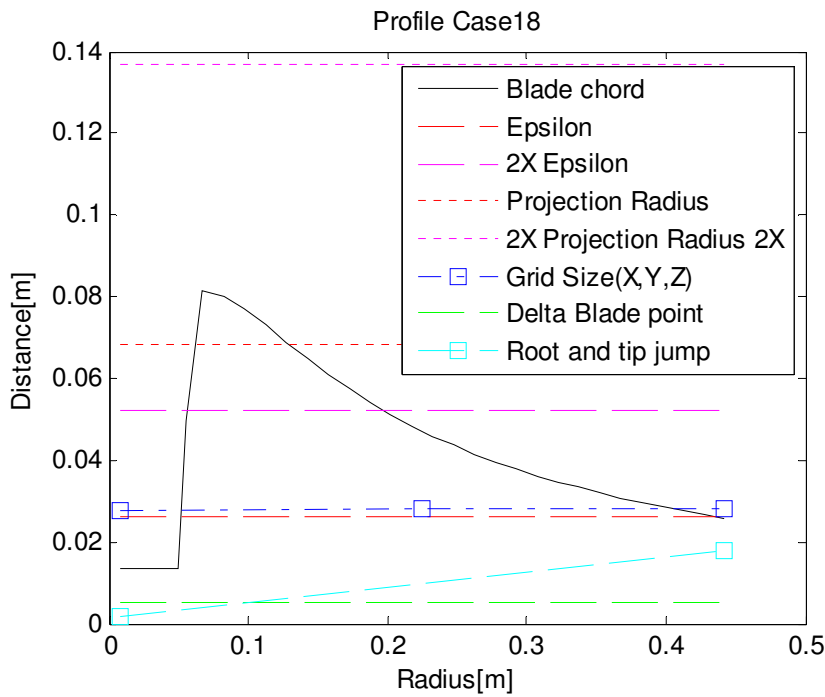


Figure 5-76 Case profile for case 18

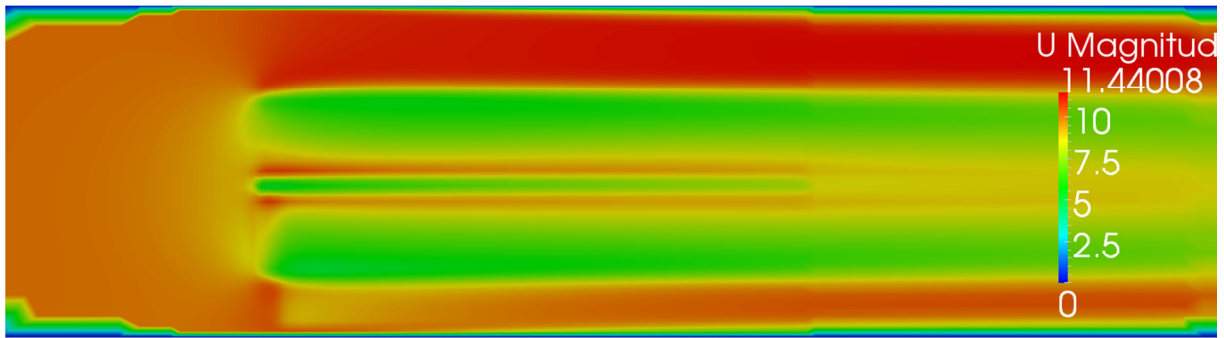


Figure 5-77 Velocity contour in the center plane through the rotor for case 18

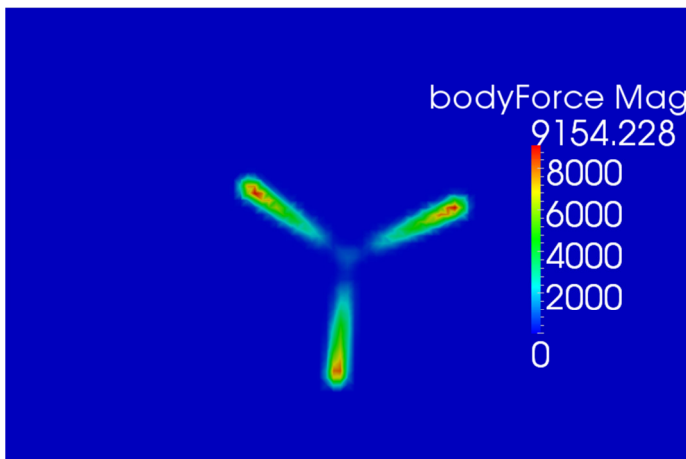


Figure 5-78 Body force distribution at the rotor plane for case 18

From Figure 5-79 we can see that the power and thrust are quite stable and close to the reference values, there are however some discretization artifacts, but not too significant.

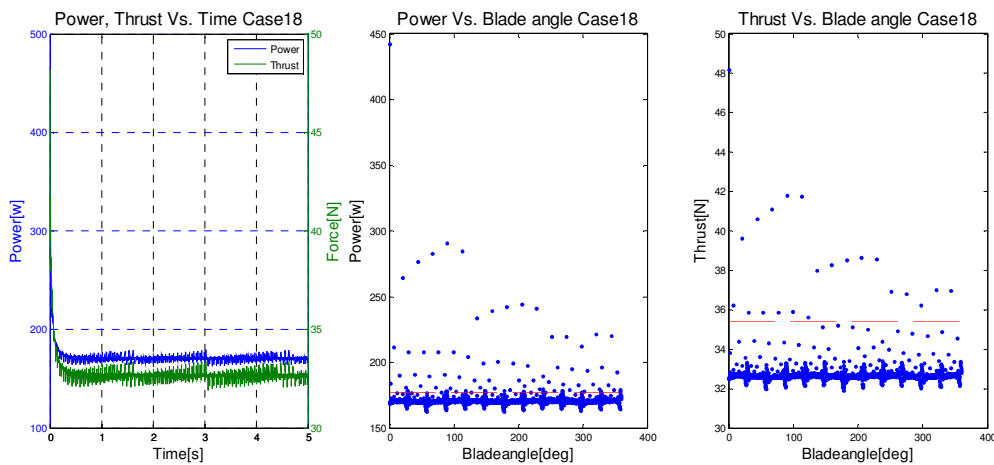


Figure 5-79 Power and thrust graphs for case 18

The velocity profiles shown in Figure 5-80 are close to the experimental data, but could be improved.

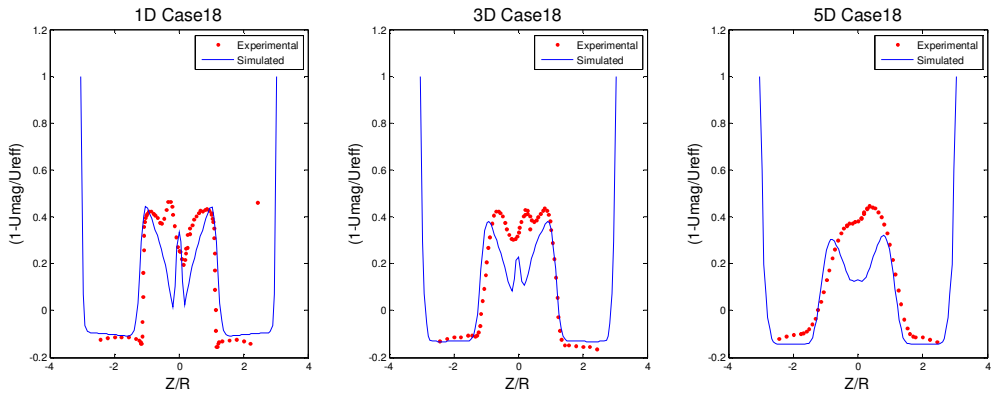


Figure 5-80 Velocity profile in the wake at 1,3 and 5 rotor diameters downstream from the rotor for case 18

6 Discussion

From the results presented in chapter 5, we can see that the epsilon factor has a significant impact on both the flow profile and the power and thrust calculations, in extreme cases like case 2 and case 6 the influence is very clear. It is interesting that both the extreme cases report far too much power and thrust. From the results it appears that there is a value of epsilon that will give a minimum power and thrust output. Case 10 was the first case to be within range of the reference. In order to achieve this the time step had to be reduced significantly, which resulted in disturbance in the calculation output. Some attempts were made to reduce the disturbance, but with limited success. To overcome this issue, modifications were made to the solver, now the solver would be implemented implicit.

The proposed new solving scheme seems to smooth out the power output, and be more stable for small time steps. This can be observed by comparing the data from case 12 with the data from case 13. The power and thrust data shown in Figure 5-60 have severe disturbance. From this data, we can see that the original solver is not sufficient to handle small time steps when the epsilon is also small. The implicit solver however handles this case much better, the power and thrust data is shown in Figure 5-63. We can see that there are some fluctuation patterns with the blade angle but far less than before. The values are also more stable, no negative values this time. However now the power and thrust output is lower than the reference. For the next cases, the time step was increased, and the epsilon factor was tuned until case 18 which were very close to the reference, and without too much disturbance.

The wake profile for case 18 could use some improvements, and was not as good as case 7, this is due to the change in the hub model, and the separate turbine approach needs more tuning in order to give the right characteristic. The focus from this study was mainly to get the power and thrust output closer to the reference.

7 Conclusion

The ALM is capable of predicting good velocity profiles, and with the implicit solver, it is also capable of calculating the power and thrust very close to the reference. However even with the new solver, the ALM is still very sensitive to parameters like epsilon, time step and grid size. It would be desirable with a force distribution model that would adapt better to different conditions. This would make the model more robust and more reliable when simulating cases without reference data to aim at.

This case might be on the limit of the intended scope of this calculation code due to the small rotor diameter and high rotational speed. Compared to full-scale wind turbines.

The influence from the hub and tower on the flow field may be model as separate actuator lines. However, more tuning is needed to get the same effect as the experimental data, a good effect was achieved by editing the blade data for the rotor, this however changed the size of the rotor and added an extra load, distorting the power calculation.

References

1. **Intrnational energy agency.** *Energy Technology Perspectives 2012.* 2012. ISBN: 978-92-64-17488-7.
2. *Numerical Modeling of Wind Turbine Wakes.* **Jens Nørkær Sørensen, Wen Zhong Shen.** s.l. : ASME, 2002, Journal of Fluids Engineering, Vol. 124.
3. *A Large - Eddy Simulation of Wind-Plant Aerodynamics .* **Matthew J. Churchfield, Sang Lee, Patrick J. Moriarty.** 2012.
4. **Troldborg, Niels.** *Actuator Line Modeling of Wind Turbine Wakes.* s.l. : Department of Mechanical Engineering, Technical University of Denmark, 2008.
5. *“Blind test” calculations of the performance and wake development for a model wind turbine.* **Krogstad, Per-Åge og Eriksen, Pål Egil.** 50, Trondheim : Elsevier Ltd., 2013.
6. **OpenFOAM wiki.** The PISO algorithm in OpenFOAM. *OpenFOAM wiki.* [Online] http://openfoamwiki.net/index.php/The_PISO_algorithm_in_OpenFOAM.
7. *Numerical Modeling of Wind Turbine Wakes.* **Sørensen, Jens Nørkær og Shen, Wen Zhong.** 2002, Journal of Fluids Engineering, Vol. 124, ss. 393-399.

Appendices

Appendix 1: Task Description

Appendix 2: Turbine Array Properties Case18

Appendix 3: Turbine Properties for Rotor Case18

Appendix 4: Turbine Properties for Hub Model Case18

Appendix 5: Turbine Properties for Tower Model Case18

Appendix 1

A “virtual” wind tunnel case set up with one model wind turbine represented with the actuator line technique is already developed and will be given to the master student as well as an introduction to the case. The model wind turbine, with the NREL s826 airfoil, has a rotor diameter of 0.89 m and the length of the virtual wind tunnel dimensions is 11 x3 x2 m. The master student will use this case as a start and perform simulations with different tips speed ratios and parameterizations and analyse the results. The results should be compared with experimental data obtained from the wind tunnel experiment at NTNU in 2011. The goal is to validate the Actuator Line model set up in OpenFOAM and to gain knowledge about the models weaknesses and strengths. Since the code is open source it is also possible to suggest improvements and code modifications.

Operate the OpenFOAM CFD code. Knowledge to CFD, C++ and OpenFOAM is an advantage but not a demand. An OpenFOAM installation guide will be given. Literature study; a study of the literature concerning wind turbine and wakes aerodynamics and the Actuator line model.

Experimenting with different parameterization of the Actuator line case. Test how the power extraction and the models ability to capture the wake aerodynamics are dependent on the grid size and other specific Actuator Line model input parameters (as the Gaussian width parameter, number of actuator segments and airfoil data) Writing a Master Thesis report and give an oral presentation.

Task background:

Disturbances in the atmosphere downstream a wind turbine can damage other turbines and will decrease efficiency in a wind farm. The region of disturbed flow is called a wake. Because of the lower wind velocity than the ambient undisturbed wind, and the often higher turbulence levels, wind farm wake effects will result in power losses and increased loading. As there are currently vast investments in offshore wind technology and because wakes offshore is shown to be more persistent than on shore wakes, wakes offshore are of particular interest. There is need for good modelling techniques for both turbine forces and wakes and this master project will concentrate on the Actuator Line method by the use of the open source CFD toolbox OpenFOAM. The master project will be connected to ongoing research activities at UiS, in StormGeo and at Acona Flow Technology.

Appendix 2

```
/*-----* C++ *-----*/
|=====|
| ¥¥ / F i e l d | OpenFOAM: The Open Source CFD Toolbox
| ¥¥ / O p e r a t i o n | Version: 1.6
| ¥¥ / A n d | Web: http://www.OpenFOAM.org
| ¥¥/ M a n i p u l a t i o n |
/*-----*/

FoamFile
{
    version      2.0;
    format       ascii;
    class        dictionary;
    object       turbineArrayProperties;
}

// *****

globalProperties
{
    outputControl    "timeStep";
    outputInterval   10;
}

turbine1
{
    turbineType      "NORCOWEBTest";
    baseLocation     (0.13 0.0 0.0);
    numBladePoints   75;
    pointDistType    "uniform";
    pointInterpType  "linear";
    bladeUpdateType  "newPosition";
    Pitch            0;
    fluidDensity     1.23;
    epsilon          0.026;
    //smearRadius     1.0;
    //sphereRadiusScalar 1.1;
    tipRootLossCorrType "glauert";
    rotationDir      "ccw";
    Azimuth          0.0;
    RotSpeed         1281.8;
    NacYaw           270.0;
}

turbine2
{
    turbineType      "HubModel";
    baseLocation     (0.13 0.0 0.0);
    numBladePoints   5;
    pointDistType    "uniform";
    pointInterpType  "linear";
    bladeUpdateType  "newPosition";
    Pitch            0;
    fluidDensity     1.23;
    epsilon          0.018;
    //smearRadius     1.0;
    //sphereRadiusScalar 1.1;
    tipRootLossCorrType "none";
    rotationDir      "ccw";
    Azimuth          0.0;
    RotSpeed         1281.8;
    NacYaw           270.0;
}
```

```
turbine3
{
  turbineType      "TowerModel";
  baseLocation     (0.26 0.000 0.0);
  numBladePoints  25;
  pointDistType    "uniform";
  pointInterpType  "linear";
  bladeUpdateType  "oldPosition";
  Pitch            0;
  fluidDensity     1.23;
  epsilon          0.030;
  //smearRadius    1.0;
  //sphereRadiusScalar 1.1;
  tipRootLossCorrType "none";
  rotationDir      "ccw";
  Azimuth          0.0;
  RotSpeed         0.0;
  NacYaw           270.0;
}
```

Appendix 3

```
/*-----* C++ *-----*/
|=====|
| ¥¥ / F i e l d | OpenFOAM: The Open Source CFD Toolbox
| ¥¥ / O p e r a t i o n | Version: 1.6
| ¥¥ / A n d | Web: http://www.OpenFOAM.org
| ¥¥/ M a n i p u l a t i o n |
|-----*/
FoamFile
{
    version      2.0;
    format       ascii;
    class        dictionary;
    object       turbineProperties;
}
// ***** //

NumBl          3;
TipRad         0.447;
HubRad         0.045;
PSPnEIN        1.0;
UndSling       0.0;
HubCM          0.0;
OverHang       -0.13;
NacCMxn        0.1;
NacCMyn        0.0;
NacCMzn        0.045;
TowerHt        0.772;
Twr2Shft       0.045;
TwrRBHt        0.0;
ShftTilt       0.0;
Delta3         0.0;
PreCone        (0 0 0);
AzimBlUp       0.0;
HubIner        100.0;
YawRate        0.0;
PitchRate      0.0;
SpeedControllerType "none";
YawControllerType "none";

//Added
GBRatio        1;
GenIner        1;
BladeIner      1;
TorqueControllerType "none";
PitchControllerType "none";

TorqueControllerParams
{
    CutInGenSpeed      670.0;
    RatedGenSpeed      1173.7;
    Region2StartGenSpeed 871.0;
    Region2EndGenSpeed 1161.963;
    CutInGenTorque     0.0;
    RatedGenTorque     43.09355E3;
    RateLimitGenTorque 15.0E3;
    KGen               2.55764E-2;
    TorqueControllerRelax 1.0;
}

PitchControllerParams
{
    PitchControlStartPitch 0.0;
    PitchControlEndPitch   7.6;
    PitchControlStartSpeed 15.77;
    PitchControlEndSpeed   16.0;
}
```

```

    RateLimitPitch      4.5;
]

//End Added

Airfoils
(
    "Cylinder2"
    "NREL_S826_RE75k"
    "NREL_S826_RE100k"
    "NREL_S826_RE150k"
);

BladeData
(
// radius(m)  c(m)      twist(deg) airfoil
( 0.0075000 0.013500 38.000 0)
( 0.022500 0.013500 38.000 0)
( 0.049000 0.013500 38.000 0)
( 0.055000 0.049500 38.000 1)
( 0.067500 0.081433 37.055 2)
( 0.082500 0.080111 32.544 2)
( 0.097500 0.077012 28.677 3)
( 0.11250 0.073126 25.262 3)
( 0.12750 0.069008 22.430 3)
( 0.14250 0.064952 19.988 3)
( 0.15750 0.061102 18.034 3)
( 0.17250 0.057520 16.349 3)
( 0.18750 0.054223 14.663 3)
( 0.20250 0.051204 13.067 3)
( 0.21750 0.048447 11.829 3)
( 0.23250 0.045931 10.753 3)
( 0.24750 0.043632 9.8177 3)
( 0.26250 0.041529 8.8827 3)
( 0.27750 0.039601 7.9877 3)
( 0.29250 0.037831 7.2527 3)
( 0.30750 0.036201 6.5650 3)
( 0.32250 0.034697 5.9187 3)
( 0.33750 0.033306 5.3045 3)
( 0.35250 0.032017 4.7185 3)
( 0.36750 0.030819 4.1316 3)
( 0.38250 0.029704 3.5439 3)
( 0.39750 0.028664 2.9433 3)
( 0.41250 0.027691 2.2185 3)
( 0.42750 0.026780 1.0970 3)
( 0.44250 0.025926 -0.7167 3)
);

```

Appendix 4

```
/*-----* C++ *-----*/
|=====|
| ¥¥ / F i e l d | OpenFOAM: The Open Source CFD Toolbox
| ¥¥ / O p e r a t i o n | Version: 1.6
| ¥¥ / A n d | Web: http://www.OpenFOAM.org
| ¥¥/ M a n i p u l a t i o n |
|-----*/

FoamFile
{
    version      2.0;
    format       ascii;
    class        dictionary;
    object       turbineProperties;
}

// *****

NumBl          3;
TipRad         0.045;
HubRad         0.001;
PSPnEIN        1.0;
UndSling       0.0;
HubCM          0.0;
OverHang       -0.13;
NacCMxn        0.1;
NacCMyn        0.0;
NacCMzn        0.045;
TowerHt        0.772;
Twr2Shft       0.045;
TwrRBHt        0.0;
ShftTilt       0.0;
Delta3         0.0;
PreCone        (0 0 0);
AzimBlUp       0.0;
HubIner        100.0;
YawRate        0.0;
PitchRate      0.0;
SpeedControllerType "none";
YawControllerType "none";

//Added
GBRatio        1;
GenIner        1;
BladeIner      1;
TorqueControllerType "none";
PitchControllerType "none";

TorqueControllerParams
{
    CutInGenSpeed    670.0;
    RatedGenSpeed    1173.7;
    Region2StartGenSpeed 871.0;
    Region2EndGenSpeed 1161.963;
    CutInGenTorque   0.0;
    RatedGenTorque   43.09355E3;
    RateLimitGenTorque 15.0E3;
    KGen             2.55764E-2;
    TorqueControllerRelax 1.0;
}

PitchControllerParams
{
    PitchControlStartPitch 0.0;
    PitchControlEndPitch   7.6;
    PitchControlStartSpeed 15.77;
    PitchControlEndSpeed   16.0;
}
```



```

    RateLimitPitch      4.5;
]

//End Added

Airfoils
(
  "Cylinder3"
//  "S826_re39000"
//  "S826_re78000"
//  "S826_re93000"
//  "S826_re101400"
//  "NREL_S826_newshort"
//  "NREL_S826_new"
//  "NREL_S826"
//  "NACA64_A17"
);

BladeData
(
//  radius(m)  c(m)    twist(deg) airfoil
( 0.0075000 0.07 38.000 0)
( 0.022500 0.07 38.000 0)
( 0.044000 0.07 38.000 0)
);

```

Appendix 5

```
/*-----* C++ *-----*/
|=====|
| ¥¥ / F i e l d | OpenFOAM: The Open Source CFD Toolbox
| ¥¥ / O p e r a t i o n | Version: 1.6
| ¥¥ / A n d | Web: http://www.OpenFOAM.org
| ¥¥/ M a n i p u l a t i o n |
|-----*/
FoamFile
{
    version      2.0;
    format       ascii;
    class        dictionary;
    object       turbineProperties;
}
// *****

NumBl          1;
TipRad         0.817;
HubRad         0.001;
PSPnEIN       1.0;
UndSling      0.0;
HubCM         0.0;
OverHang      -0.13;
NacCMxn       0.1;
NacCMyn       0.0;
NacCMzn       0.045;
TowerHt       0.001;
Twr2Shft     0.045;
TwrRBHt       0.0;
ShftTilt      0.0;
Delta3        0.0;
PreCone       (0 0 0);
AzimBlUp     0.0;
HubIner       100.0;
YawRate       0.0;
PitchRate     0.0;
SpeedControllerType "none";
YawControllerType  "none";

//Added
GBRatio       1;
GenIner       1;
BladeIner     1;
TorqueControllerType "none";
PitchControllerType  "none";

TorqueControllerParams
{
    CutInGenSpeed    670.0;
    RatedGenSpeed    1173.7;
    Region2StartGenSpeed 871.0;
    Region2EndGenSpeed 1161.963;
    CutInGenTorque   0.0;
    RatedGenTorque   43.09355E3;
    RateLimitGenTorque 15.0E3;
    KGen             2.55764E-2;
    TorqueControllerRelax 1.0;
}

PitchControllerParams
{
    PitchControlStartPitch 0.0;
    PitchControlEndPitch   7.6;
    PitchControlStartSpeed 15.77;
    PitchControlEndSpeed   16.0;
}
```

```

    RateLimitPitch      4.5;
]

//End Added

Airfoils
(
    "Cylinder2"
    "S826_re39000"
//    "S826_re78000"
//    "S826_re93000"
//    "S826_re101400"
//    "NREL_S826_newshort"
//    "NREL_S826_new"
//    "NREL_S826"
//    "NACA64_A17"
);

BladeData
(
// radius(m)  c(m)      twist(deg) airfoil
//( 0.001 0.102 38.000 0)
( 0.001 0.102 38 0)
( 0.177 0.102 38 0)
( 0.178 0.082 38 0)
( 0.416 0.082 38 0)
( 0.417 0.061 38 0)
( 0.576 0.061 38 0)
( 0.577 0.051 38 0)
( 0.817 0.051 38 0)
( 0.818 0.001 38 1)
);

```